THERMAL REGENERATION OF BIOCHAR FOR ADSORPTION OF SYNTHETIC ORGANIC CONTAMINANTS IN THE PRESENCE OF DISSOLVED ORGANIC MATTER

by

BENJAMIN GLENN GREINER

A thesis submitted to the

Faculty of the Graduate School of the

University of Colorado Boulder

in partial fulfillment of the requirement for the degree of

Master of Science

Department of Civil, Environmental, and Architectural Engineering

2017

This thesis entitled:

Thermal Regeneration of Biochar for Adsorption of Synthetic Organic Contaminants in the Presence of Dissolved Organic Matter

written by Benjamin Glenn Greiner

has been approved for the Department of
Civil, Environmental, and Architectural Engineering

R. Scott Summers

Karl G. Linden

Fernando Rosario-Ortiz

Date: _____

The final copy of this thesis has been examined by the signatories, and we find that both the content and the form meet acceptable presentation standards of scholarly work in the above mentioned discipline.

Greiner, Benjamin Glenn (B.S./M.S., Civil Engineering [Department of Civil, Environmental, and Architectural Engineering])

Thermal Regeneration of Biochar for Adsorption of Synthetic Organic Contaminants in the Presence of Dissolved Organic Matter

Thesis directed by Professor R. Scott Summers

Abstract

Biochar is emerging as a cost effective carbonaceous adsorbent for removing pollutants such as synthetic organic contaminants (SOCs) from wastewater, stormwater, and drinking water sources. However, relative to commercial activated carbon (AC), biochar fouls rapidly when applied in a flow-through column in the presence of background dissolved organic matter (DOM). Thermal regeneration is a promising process for regaining adsorption capacity in fouled biochar. In this study, 850 °C pine biochar was fouled in a column with environmentally relevant concentrations of sulfamethoxazole (SMX) and DOM, then heated in a second semi-oxic thermal regeneration step at 600 °C. The treatment resulted in a dramatic improvement in SMX column adsorption capacity in the presence of DOM. DOM adsorption capacity was also improved. The treatment was applied to fresh char that had not been fouled, and the improvement in adsorption capacity was still observed. This increase in adsorption capacity was strongly correlated with an observed increase in BET surface area and decrease in average pore diameter, and was still significant even after accounting for the decrease in mass of char during the heating step. The improvement in adsorption capacity and increase in surface area was repeatable for multiple cycles of fouling and regeneration, although the further increase in adsorption capacity in the second regeneration cycle was counteracted by the loss of mass of char. While the adsorption capacity of biochar for SMX in the presence of DOM was greatly improved by the second heating step, it still did not approach the capacity of the activated carbon. A positive effect of

empty bed contact time (EBCT) on SMX adsorption capacity was observed for biochar after the regeneration/enhancement heating step, and for activated carbon, but not for fresh biochar. A change in particle size distribution was not observed due to the reheating process.

Acknowledgements

I would like to thank my advisor, R. Scott Summers, for his guidance and support in this research and for his infectious enthusiasm for working on interesting problems with great people. I would also like to express my gratitude to Kyle Shimabuku for his encouragement to pursue research on the thermal regeneration of biochar, his willingness to share his expertise in the lab, his patience for having the same conversations over and over, and his joyful approach to science and life. Thanks to Josh Kearns for his unwavering vision for the future of biochar, and his relentless dedication to the bigger picture. Thanks to Matt Bentley and Chris Corwin for their help in brainstorming approaches and interpretations, and for general companionship. Thanks to Riley Mulhern for sharing his expertise with RSSCT operation. Thanks to Dorothy Noble, Leigh Gilmore Terry, Kyle Thompson, and the rest of the rotating cast of characters in the Summers Lab group who helped fine tune presentations and cross examine my explanations. Thanks to my committee members, Karl Linden and Fernando Rosario-Ortiz, for their insight and cross-examination of this work.

Thanks to my parents for getting me excited about science and encouraging me to follow whatever path I saw for myself. Also, a huge thank you goes to the rest of my family and friends for supporting me in this whole pursuit, and tolerating my strange schedules of lab work and RSSCT sampling. Thank you for believing in me and encouraging me!

I would like to acknowledge the funding support of the Mortenson Center in Engineering for Developing Communities, the Norlin Scholars program, and WateReuse Colorado.

Contents

List of Tables

List of Figures

1. INTRODUCTION

Chemical pollution of water from anthropogenic sources has been widely recognized as a human health risk in the world's wealthy nations for decades (1). Insecticides, herbicides, chlorinated solvents, and brominated compounds are included in this broad range of harmful chemical pollutants. More recently, pharmaceuticals and personal care products (PPCPs) have emerged as potential areas of concern, including endocrine disrupting compounds, both for their potential ecosystem impacts and influences on human health (2–5). Disinfection byproducts (DBPs), which are created when chlorine reacts with dissolved organic matter, have also emerged as widely-occurring contaminants with potential carcinogenic and reproductive health effects (6–8). This wide swath of chemical pollutants, including insecticides, herbicides, PPCPs, and DBPs, can be broadly categorized as synthetic organic contaminants (SOCs). Many of the compounds of concern are recalcitrant to biodegradation, and are not significantly affected by traditional water treatment or conventional activated sludge treatment of wastewater (9,10). Further, synthetic organic contaminants can often be introduced into the environment through stormwater runoff or combined sewer overflows (11,12), and so bypass treatment altogether.

In the global context, microbial contamination of waters has been the primary focus of the water, sanitation, and hygiene (WASH) sector in low- and middle-income countries, largely leaving chemical contamination out of the conversation. However, chemical pollution is gaining traction as an important health threat facing developing communities (13,14). Products such as pesticides that are more tightly regulated in high income countries can often be stockpiled or used extensively in low- and middle-income countries due to lax environmental regulation and poor education about the risks of exposure (14). Additionally, the bulk of pharmaceutical manufacturing and e-waste disposal occurs in these countries, contributing to extensive chemical

pollution of water sources in countries like India and China, which poses an enormous risk to public health (13,14).

When possible and economical, treatment by adsorption to activated carbon (AC) has emerged as a primary control strategy of SOCs (15–18). AC is a good adsorbent due to its surface properties, and extensive internal surface area (15). However, AC can be an inappropriate solution for reasons of production cost and transport (11), depending on the context of the application.

Biochar has been proposed as an appropriate alternative to AC in some situations, such as wastewater and drinking water treatment in low income or remote communities and stormwater outfalls as a barrier to environmental degradation (11,13). Biochar is a carbonaceous material that is produced by pyrolysis of organic feedstock, and can have similar adsorption properties to granular AC (GAC) if production conditions are optimized for adsorption (19,20). Pyrolysis occurs at high temperatures in a limited-oxygen environment. The peak temperature of pyrolysis has been shown to be a key parameter in the adsorption capacity of biochar, with biochar produced at a peak temperature of 850 °C performing similarly to powdered AC (PAC) in batch equilibrium tests in one study (11). Internal surface area of biochar has previously been reported to be as high as 500 m^2/g for biochars without feedstock pretreatment (11,20), and this large amount of surface area facilitates high adsorption capacities. Low-cost gasifier drum ovens, termed top-lit updraft (TLUD) gasifiers, have been shown to produce high-quality biochar in a mode accessible to developing communities, allowing for distributed production using a range of locally available feedstocks (19,21). Biochar can be produced using locally available feedstocks and technologies, which means that it could be widely applied in low and middle income countries to minimize the human health risk of exposure to SOCs. Its cheaper production cost

may mean that biochar could also be an appropriate technology to minimize release of SOCs into the environment even in high income countries in situations where AC is not economical (11).

Although biochar can perform well in batch equilibrium sorption in laboratory clean water, it fouls much more rapidly than AC in the presence of background dissolved organic matter (DOM) (11). DOM is comprised of dissolved natural organic matter (NOM) produced by the degradation of vegetable and animal matter in the environment, and anthropogenic organic matter discharged to the water (1). Dissolved organic carbon (DOC) concentration and ultraviolet absorbance (UVA) are used as primary characterizing parameters for DOM concentrations in water (15). DOM concentrations have been found to significantly affect the efficacy of GAC as a treatment for SOCs (22,23). DOM can compete with SOCs for adsorption sites, as well as block macropores, which decreases the available surface area for sorption (24).

Column operation is important to characterize when DOM is present in the water matrix, because it can break through prior to the contaminant of interest. This has a pre-fouling effect on much of the lower carbon in a column, leading to pore blockage and lower-than-expected capacity for the contaminant of interest (24).

Rapid small-scale column tests (RSSCTs) are physically-scaled models that are used to characterize the performance of carbonaceous adsorbents in column mode, and their results have been applied to predict full-scale breakthrough of target compounds, such as DOC and various organic compounds (25). However, they do not assess biological degradation processes that can be present at the full scale (15,25). By holding constant some of the non-dimensional numbers that describe the mass transfer and flow regime in a full-scale column, the column size and operation time can be scaled down to allow much more rapid determination of breakthrough curves. There are two general approaches to design of RSSCTs: constant diffusivity (CD) and

proportional diffusivity (PD). For CD, it is assumed that the intraparticle diffusivity of the target compound is constant and independent of particle size. This design assumption can lead to high head loss and operational difficulties due to a high flow rate. It has been found that for some compounds and flow regimes, assuming that intraparticle diffusivity scales proportionally with particle diameter leads to more satisfactory results and easier RSSCT operation (26,15,25).

Using the PD design assumptions, it can be shown that the empty bed contact time (EBCT) and operation time (*t*) are scaled by the ratio of particle diameter (*d*), as shown in the equation below, where SC is the small column and LC is the large column (26):

$$\frac{EBCT_{SC}}{EBCT_{LC}} = \frac{t_{SC}}{t_{LC}} = \frac{d_{SC}}{d_{LC}}$$

GAC is often regenerated or reactivated by various methods once its adsorption capacity has been exhausted (27). Regeneration is defined by regaining adsorption capacity without changing the original structure of the adsorbent, while reactivation usually involves additional oxidation to access new surface area, using some activation agent such as steam or air (15,27). One of the simplest methods of regeneration of carbonaceous adsorbents is thermal regeneration, wherein the adsorbent is heated in order to decompose and remove the various constituents that are occupying adsorption sites on the surface (27). When thermal regeneration is performed on activated carbon, it is generally not possible to recover all of the original absorption capacity, and some loss of capacity compared to the fresh carbon is expected (28), which is why reactivation is most commonly used in water treatment for GAC (15). Compounds that desorb from the surface of the carbon usually degrade to some extent in the process of desorption (15,29), and may even combust completely in the effluent gas stream that is created, decreasing the danger of re-releasing sorbed compounds back into the aqueous environment when it is time to dispose of the spent adsorbent. That said, gaseous byproducts of thermal regeneration and

reactivation can have deleterious effects on the atmosphere and human health, and so care should be taken to treat gas streams prior to releasing them into the environment (24). Mass yield of regeneration processes is also of concern. For activated carbons, minimal mass loss has been observed when the regeneration is conducted in an inert atmosphere at a lower temperature than was used to initially generate the adsorbent, although higher temperatures were necessary to achieve regeneration, which resulted in mass loss (30).

Regeneration and reactivation of AC are accepted strategies to improve economic viability of the technology and minimize risk associated with disposing used AC that could lead desorption of contaminants back into the environment (15). Biochar adsorbents face the same challenges, but regeneration of biochar has not been widely studied. Thermal regeneration is a promising prospect for regeneration of adsorption capacity of biochars. The goal of the present study is to evaluate the effectiveness of thermal regeneration of biochar for adsorption of SOCs at environmentally relevant concentrations in the presence of DOM. The main characteristics of concern in assessing the effectiveness of a regeneration process are the mass yield and specific adsorption capacity. If a process recovers adsorption capacity, but results in a greatly decreased mass of adsorbent, then it is less likely to be economically beneficial. Thus, this study aimed to assess both of these factors in the thermal regeneration of biochar. The temperature and duration of thermal regeneration were chosen in order to approximate a process that may be possible to conduct using waste heat from pyrolysis of fresh feedstock using something akin to the JRO-TLUD oven (31), which would allow the application this process in a distributed fashion in low- and middle-income countries. Such an application of thermal regeneration could improve economic viability of biochar and minimize problems associated with disposal of used biochar.

Sulfamethoxazole (SMX) is used in this study as a test compound to characterize adsorption capacity of carbonaceous adsorbents (biochar and AC) for SOCs. SMX is a widely used human and veterinary antibiotic, which has been detected in wastewater effluent, surface waters, and groundwater throughout the world (4,32,33). It has a molecular weight of 253.3 g/mol (34), is anionic at neutral pH with a $pKa_{,2}$ of 5.7 (35), is relatively resistant to photodegradation (35), is recalcitrant to biodegradation (36), and is relatively poorly adsorbed by carbonaceous adsorbents (37). These properties make SMX persistent in the environment, and a good indicator compound for the performance of biochar sorbents. If an adsorbent can remove SMX, then it can likely remove many other SOCs (18,10). Additionally, SMX is a good indicator adsorbate for evaluating the efficacy of regeneration processes. One study by Suzuki et al. found that the boiling point and ratio of aromatic carbon to total carbon in an organic compound was related to the ease of desorption by thermal regeneration processes (29). They developed three groups of organic compounds characterized by differing difficulties of removal from activated carbon by thermal regeneration. By these criteria, SMX is part of group III, which is “not easily removed by heating only”. Thus, if a thermal regeneration process works for adsorbents exhausted for SMX adsorption, it is likely to work for many other compounds.

2. METHODS

Process overview

An overview of the processing of various adsorbents is depicted in Figure 2.1.

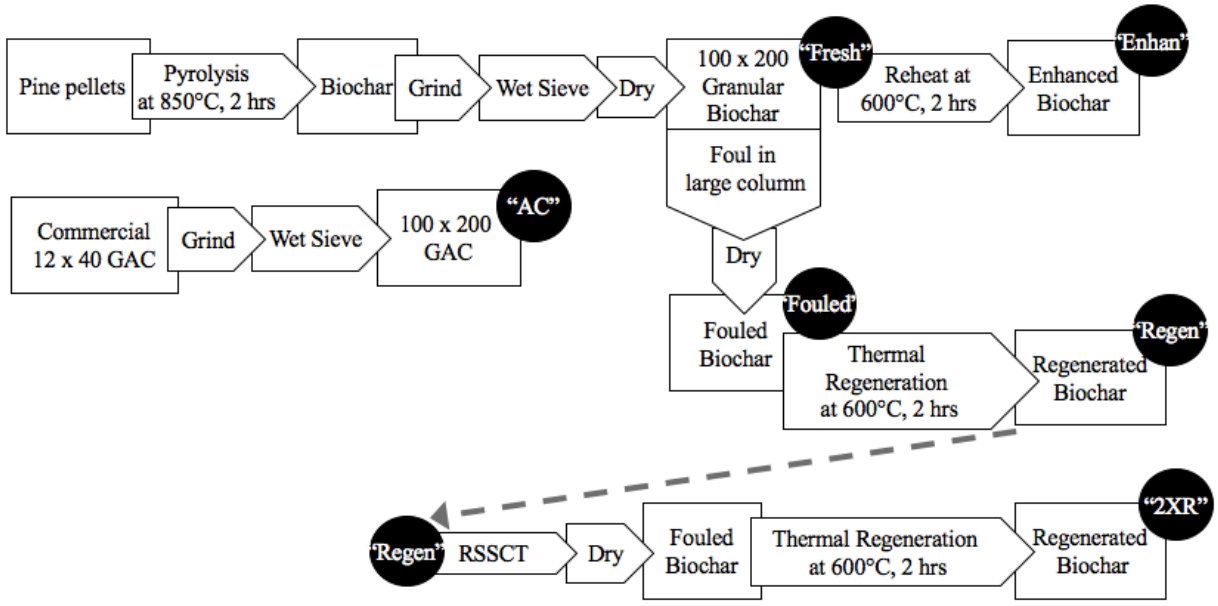

Figure 2.1: Process flow diagram. Black circles indicate adsorbent (biochar or activated carbon) that is used as media in an RSSCT.

Char Preparation

Biochar was produced from pelletized pine forestry waste (Black Hills GOLD, Spearfish Pellet Company LLC, Spearfish, SD). Pellets were packet into cylindrical ceramic crucibles (4 inches in diameter, 2.5 inches deep) and closed with as little headspace as possible. The pine pellet feedstock was then pyrolyzed in a laboratory muffle furnace, with a peak temperature of 850°C, maintained for 2 hours. The heating rate was 10 °C/min. Char was ground with a mortar and pestle, and wet sieved using reverse osmosis-produced water (RO). The size fraction of particles retained was that which passed a standard 100 mesh sieve (150 µm opening) and was

retained on a standard 200 mesh sieve (75 μm opening). Char was then decanted in order to remove residual fines. This 100 x 200 biochar was dried at ~80°C overnight in order to assess the efficiency of grinding and sieving. Char that had been processed to this point is referred to as "fresh" biochar in figures and further discussion. Mass yields for each grinding and sieving session are included in Table 2.1.

Table 2.1: Mass yields for char and GAC grinding and wet sieving handling.

Process	Mass Yield	Used in RSSCT
Char Grind/Sieve	48.1%	Fouled, Regenerated, 2XR
Char Grind/Sieve	38.6%	Fresh, Enhanced
GAC Grind/Sieve	33.2%	AC

Approximately 62 g of "fresh" biochar was loaded in a glass column with cross-sectional area of 1 cm^2, and used to treat a stream of the chosen water matrix at various flow rates until the effluent SMX concentration was 88% of the influent concentration. The char was moved to a different column with a cross sectional area of 6 cm^2 part way through fouling in order to increase the hydraulic loading rate without causing excessive head loss. When full breakthrough was observed, the char was removed from the column and dried at ~80°C overnight. Char that had been processed to this point is referred to as "fouled" biochar in figures and further discussion, and an aliquot was characterized in an RSSCT column test in order to verify the extent of fouling.

"Fouled" biochar was mixed and split into 7 aliquots by a scaled down version of the coning and splitting sampling method described by Bucheli et al. (38). Each aliquot was 7.5±0.3 g of char (dry mass). One aliquot was split into two Fisherbrand FB-965-D ceramic crucibles, with 15 mL capacity each, and covered. The crucibles contained about 30% headspace by volume. One aliquot of fouled char was then thermally regenerated in a laboratory muffle

furnace, with a peak temperature of 600°C maintained for 2 hours. Other aliquots were also thermally regenerated with a peak temperature of 700°C and 850°C for two hours, but further analysis was not conducted with these aliquots. A small layer of ash was observed on each sample after thermal regeneration, indicating a small amount of full combustion, which likely contributed to the majority of mass loss observed. The total amount of ash was negligible by mass percentage, and was removed from the samples with a light puff of air. Any residual ash was not considered problematic because it has been demonstrated that ash has negligible SMX adsorption capacity (11). Char that had been processed to this point is referred to as "regenerated" biochar in figures and further discussion.

Mass yields from pyrolysis and thermal regeneration processes are listed in Table 2.2.

Table 2.2: Char yield of pyrolysis, first and second regeneration cycles, enhancement reheat cycle and grinding/sieving.

Process	Temperature (°C)	Mass Yield	Used in RSSCT
Pyrolysis	850	21.5%	All
Regeneration	600	85.4%	Regenerated, 2XR
Regeneration	700	78.3%	-
Regeneration	850	70.1%	-
2nd Regeneration	600	75.0%	2XR
Enhancement Reheat	600	80.2%	Enhanced

In order to isolate the effect of fouling prior to thermal regeneration, an aliquot of "fresh" biochar was processed in the same manner as the "fouled" biochar. 5.95 g of char was placed into two covered Fisherbrand FB-965-D ceramic crucibles with approximately 30% headspace, and heated in a laboratory muffle furnace with a peak temperature of 600°C, maintained for 2 hours. A similar layer of ash was observed and removed. Char that had been processed to this point is referred to as "enhanced" biochar in figures and further discussion. It differs from

"regenerated" biochar because it had not been exposed to the water matrix prior to the second heating process.

In order to compare biochar performance to that of activated carbon, a sample of Norit 1240 GAC was ground using a mortar and pestle, and wet sieved to attain a 100 x 200 mesh size. This GAC was dried at ~80°C overnight in order to assess the efficiency of grinding and sieving. This carbon is labeled "AC" in further figures.

All adsorbents were loaded into RSSCT columns, the design of which is discussed below, and used to treat the chosen water matrix. When the "regenerated" biochar had again broken through such that the effluent SMX concentration from the 20 minute EBCT column was >80% of the influent SMX concentration, char from the first two column sections was dried overnight at ~80°C, yielding 2.60g. This char was then placed in a covered Fisherbrand FB-965-D ceramic crucible, and thermally regenerated in a laboratory muffle furnace with a peak temperature 600 °C, maintained for two hours. Again, a small layer of ash was observed and removed. Char that had been processed to this point is referred to as "twice regenerated" biochar in figures and further discussion, abbreviated as "2XR".

Water Matrix

Water that was circulated through the large fouling column and RSSCTs was prepared using water from Big Elk Meadows Lakes, near Lyons, Colorado (BEM) and RO water, targeting 4 mg/L TOC, then spiked with ~200 ng/L of SMX. BEM water was first filtered through a 0.45 μm filter. Influent samples were taken concurrently with each effluent sample from the RSSCTs, and the average characteristics of the resulting water matrix are shown in Table 2.3.

Table 2.3: Average influent water characteristics for large fouling column and RSSCT's. pH value shown is based on one measurement.

TOC (mg/L)	UVA_{254nm} (cm^{-1})	pH	C_{SMX} (ng/L)
4.18	0.100	7.88	191

Breakthrough of TOC, $UVA_{254\ nm}$, and SMX were monitored at the intermediate sample points and the effluent of each RSSCT. ^{14}C-labeled SMX was obtained from American Radiolabeled Chemicals, Inc. (St. Louis, MO), and its concentration was measured using a Tri-Carb 2300TR liquid scintillation counter. TOC was analyzed using a Sievers 5310C Laboratory TOC Analyzer, and UVA_{254nm} was analyzed using a Hach DR/4000U Spectrophotometer.

RSSCT Design and Operation

The RSSCTs were designed using the assumptions of proportional diffusivity (26,39,40). A flow rate of 2 mL/min was targeted, using a Cole Parmer model 7090-62 PTFE Diaphragm pump, rated for 100mL/min at 0 psi, 75 psi max continuous duty, and 400 RPM continuous duty, attached to a Cole Parmer Masterflex Console Drive. Empty bed contact times ($EBCT_{LC}$) were chosen as shown in Table 2.4 for each sample. The exact mass transfer scaling was not considered crucial in this design process, because the goal was to directly compare the performance of the different adsorbents, rather than to predict full scale performance.

Table 2.4: Chosen EBCTs for RSSCTs.

Adsorbent	**$EBCT_{LC}$**		
	10 min	**20 min**	**30 min**
Fresh Biochar	X	X	X
Fouled Biochar		X	
Regenerated Biochar	X	X	X
Twice Regenerated (2XR) Biochar	X		
Enhanced Biochar	X	X	
Activated Carbon	X	X	

The Teflon tubing used had an internal diameter of 0.476 cm, which led to a bed length of 13.22 cm per 10 minutes of EBCT. When multiple EBCTs were evaluated for a given adsorbent, intermediate sample points were established in a series of 10 minute $EBCT_{LC}$ columns, as shown in Figure 2.2.

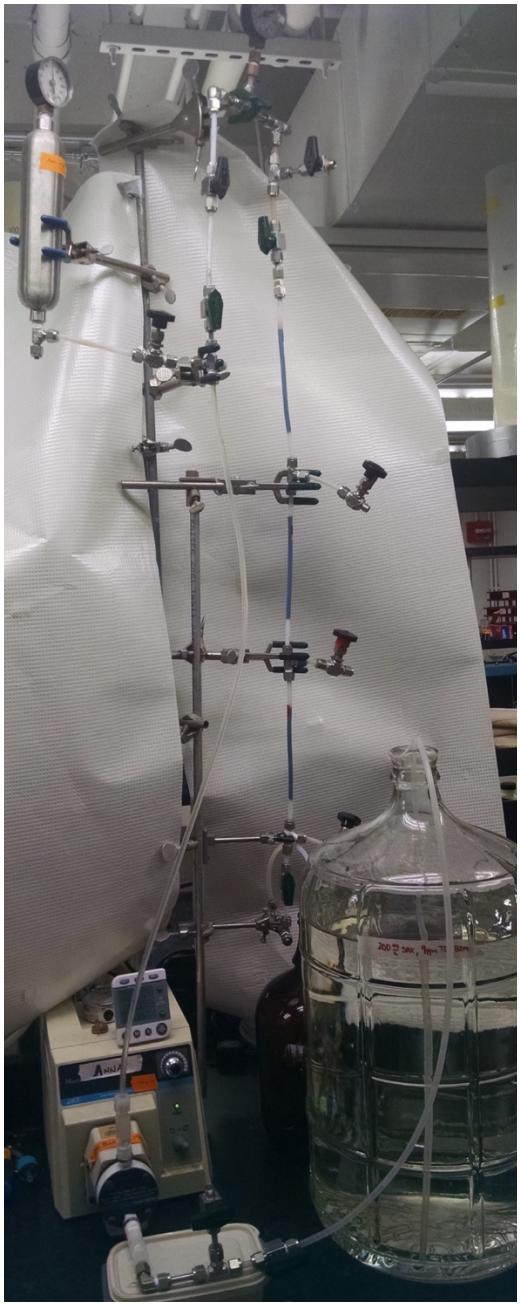

Figure 2.2: RSSCT Experimental Setup with influent, 10 min, 20 min, and 30 min $EBCT_{LC}$ sampling ports.

A pulsation damper chamber was attached to the system downstream of the pump, followed by a glass wool filter, air release valve, and sampling point for influent samples. Adsorbent beds followed this sampling point, separated by glass wool plugs if multiple beds were in series. A p-trap configuration was attached to the system downstream of the last adsorbent bed in order to keep air bubbles from travelling up the tube into the adsorbent.

To load the adsorbent beds, char was submerged in RO water, and degassed in a vacuum chamber at least overnight before the slurry was loaded into the tubing using a pipettor. All columns were operated at room temperature (20°C-24°C).

Column flow rate was calculated regularly according to volume passed and time elapsed, and pumps were adjusted as necessary. The resulting average flow rate was 2.00±0.26 mL/min. Samples were discarded if flow rate during sampling differed from the target flow rate by more than 10% (0.2 mL/min). After any flow rate adjustments, the column was allowed to equilibrate for at least 10 bed volumes prior to sampling, in order to more closely match steady state operation.

BET Surface Area and Particle Size Distribution

BET (Brunauer, Emmet, and Teller) surface area analysis and BJH (Bennett, Joyner, and Halenda) pore size distribution analysis of biochar samples were conducted using Micromeritics Gemini VII Model 2380 Surface Area Analyzer, using nitrogen as the adsorbate. Particle size distribution was analyzed using a Mastersizer Hydro SM2000(a) instrument.

3. RESULTS

Breakthrough of Sulfamethoxazole on Fresh, Fouled, and Regenerated Adsorbents

Breakthrough results for SMX are shown as normalized concentration, the ratio of effluent effluent concentration to the average influent concentration, as a function of throughput in bed volumes, which can be calculated at the ratio of operation time to EBCT, or volume treated to adsorbent bed volume, in **B)**

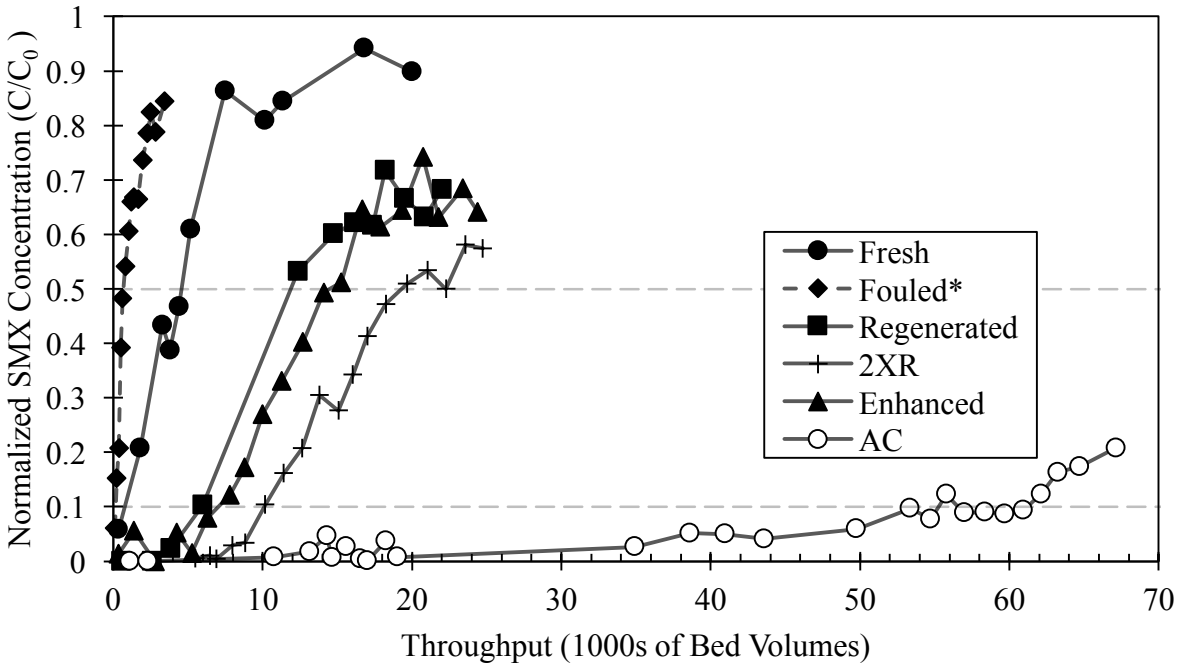

Figure 3.1, Figure 3.2, and Figure 3.3, for the 10-, 20-, and 30-min EBCTs, respectively. The average influent SMX concentration was 191 ng/L.

Char that was thermally regenerated not only regained its previous adsorption capacity for SMX, but exhibited a dramatic increase in adsorption capacity, at all three EBCTs. This effect was also observed in the enhanced char, and so the increase in capacity was independent of whether the char had been previously used or not. Previous use appeared to slightly decrease the improvement at the 10-minute empty bed contact time, but no samples were obtained

between 10% and 50% SMX breakthrough, and so the evidence for this conclusion is tenuous. Enhanced and regenerated biochar behaved nearly identically at the 20-minute EBCT. The second round of thermal regeneration added even further adsorption capacity, leading to later breakthrough of SMX at the 10-minute EBCT. Despite these improvements in biochar adsorption capacity, activated carbon still significantly outperformed any biochar. The RSSCT using fouled biochar verifies that adsorption capacity of the char was indeed greatly reduced prior to thermal regeneration.

A)

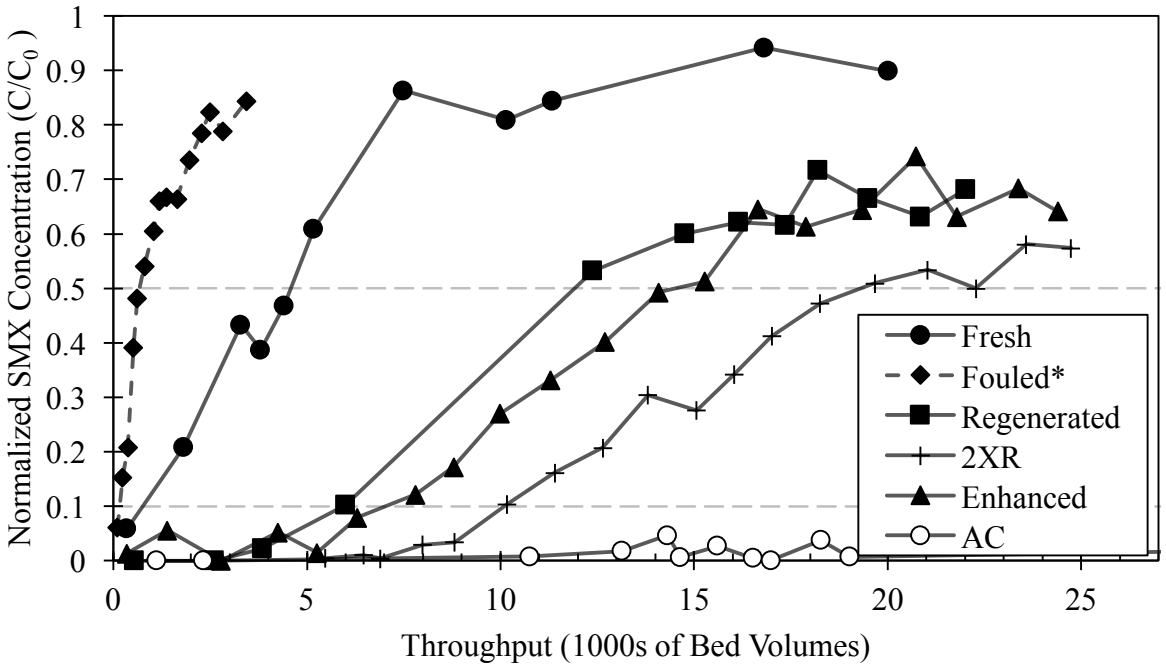

B)

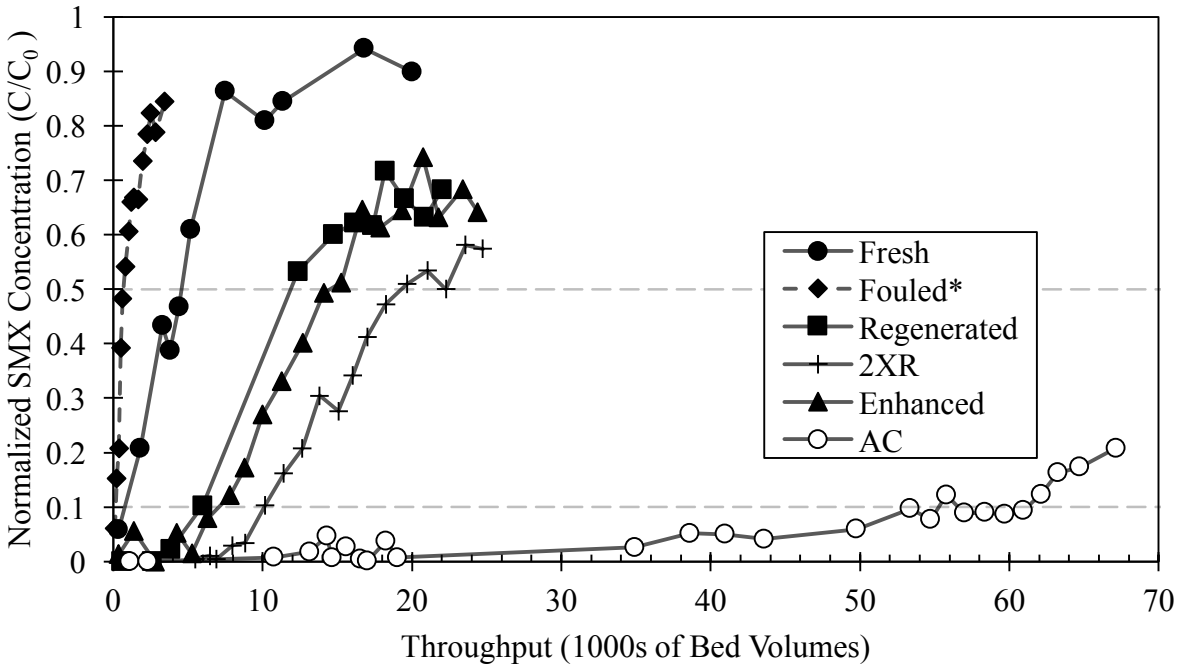

Figure 3.1: A) Breakthrough of sulfamethoxazole (SMX) for various adsorbents for large column empty bed contact time of 10 minutes ($EBCT_{LC}$), and B) The same figure expanded to show SMX breakthrough for AC.
** Fouled adsorbent is shown for $EBCT_{LC}$ of 20 minutes.*

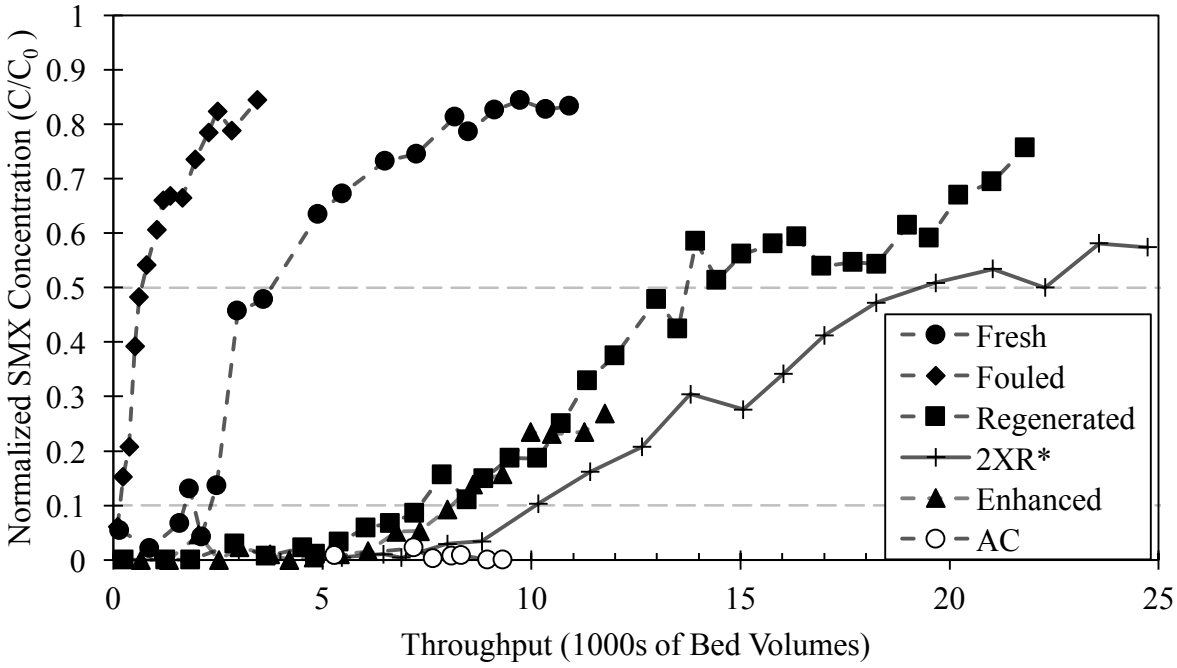

*Figure 3.2: Breakthrough of sulfamethoxazole (SMX) for various adsorbents for large column empty bed contact time of 20 minutes ($EBCT_{LC}$). *Twice-regenerated biochar (2XR) is shown for $EBCT_{LC}$ of 10 minutes.*

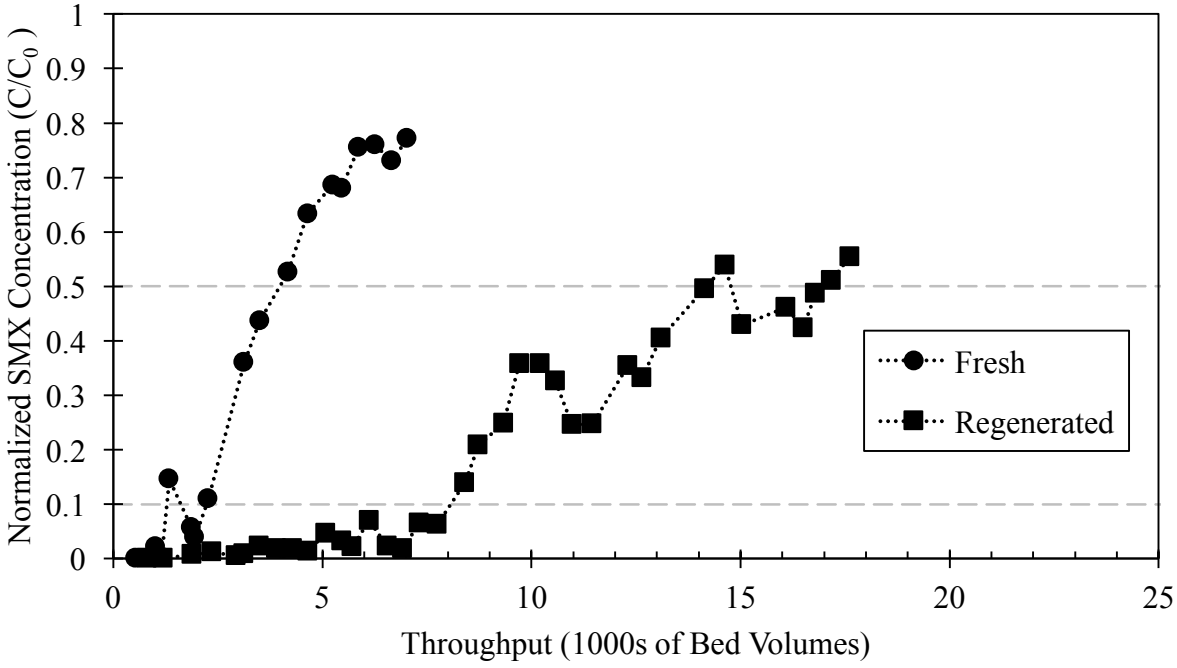

Figure 3.3: Breakthrough of sulfamethoxazole (SMX) for fresh and regenerated biochar with a large column empty bed contact time ($EBCT_{LC}$) of 30 minutes.

Adjusting for Mass Losses

The approximate bed volumes at 10% SMX breakthrough (BV_{10}), and 50% breakthrough (BV_{50}) for each adsorbent are displayed in Table 3.1. Also displayed are the bed volumes to breakthrough multiplied by the total efficiency of thermal regeneration, η_{total}, as a measure of adsorption capacity per mass of fresh biochar. Total efficiency is defined as the product of mass yields for thermal regeneration cycle undergone by the char, which are displayed in Table 2.2. Even when adjusted for the mass losses incurred during thermal regeneration and enhancement, the regenerated and enhanced biochar perform better than fresh biochar. In the second regeneration cycle, most of the additional benefit beyond the first cycle is counteracted by mass loss, but the improvement over fresh char is maintained. This is visually demonstrated by the presentation of the same data in Figure 3.4.

Table 3.1: Approximate bed volumes to 10% and 50% SMX breakthrough, bed volumes to SMX breakthrough adjusted for regeneration mass yield, and bed volumes to 80% UVA_{254} breakthrough for various adsorbents.

Adsorbent	**SMX**				**UVA_{254}**
	BV_{10}	**BV_{50}**	**$BV_{10}*\eta_{total}$**	**$BV_{50}*\eta_{total}$**	**BV_{80}**
Fresh	1,500	4,100	1,500	4,100	700
Fouled	150	620	-	-	100
Regenerated	7,100	14,000	6,100	12,000	2,100
2XR	10,000	19,200	6,400	12,300	2,900
Enhanced	7,400	14,800	5,900	11,900	1,600
GAC	56,000	-	-	-	24,000

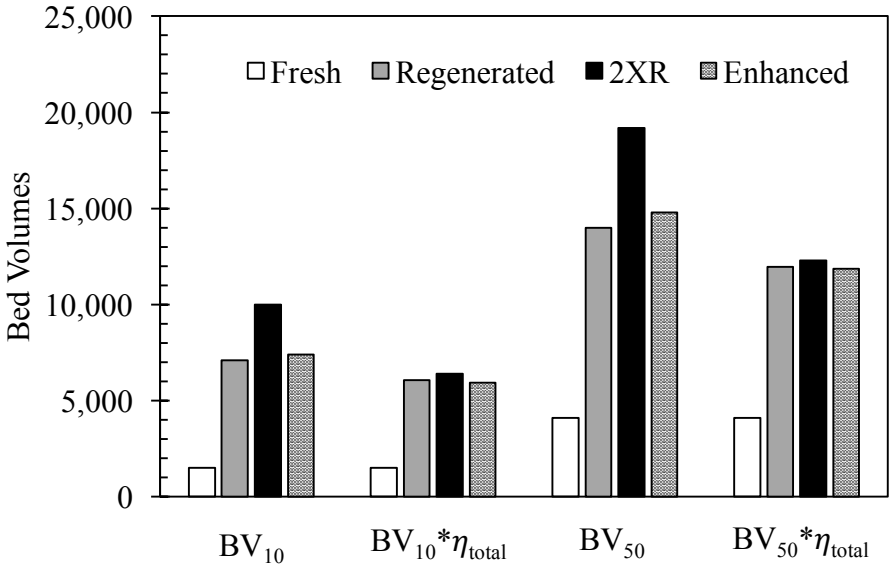

Figure 3.4: Bed volumes to 10% and 50% SMX breakthrough, and bed volumes to breakthrough adjusted by total regeneration efficiency.

Effect of Empty Bed Contact Time on SMX Breakthrough

The impact of EBCT on SMX breakthrough is shown in Figure 3.5 and Figure 3.6. For fresh biochar, very little-to-no effect of EBCT was observed on SMX breakthrough (Figure 3.5). The shorter empty bed contact time seemed to lead to faster breakthrough earlier on, which then crosses over with longer EBCTs around 3,000 bed volumes. This is consistent with previous results using activated carbon from Corwin and Summers, who attributed the effect to the pre-fouling effect of DOM, which has a longer mass transfer zone than the more strongly-adsorbed organic contaminants (17). A slight effect was observed for regenerated char, shown in Figure 3.5, and enhanced char, shown in Figure 3.6, where shorter EBCTs had earlier SMX breakthrough. However, the crossover was never clearly observed.

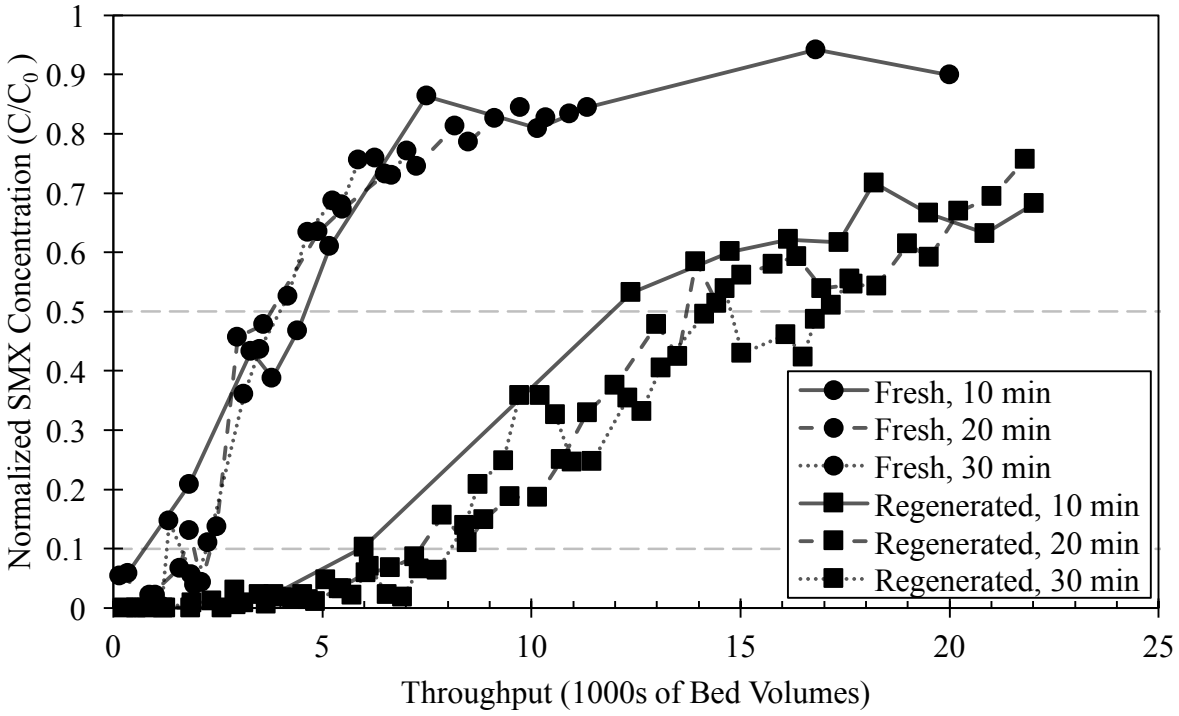

Figure 3.5: Effect of empty bed contact time ($EBCT_{LC}$) on SMX breakthrough for fresh and regenerated biochar.

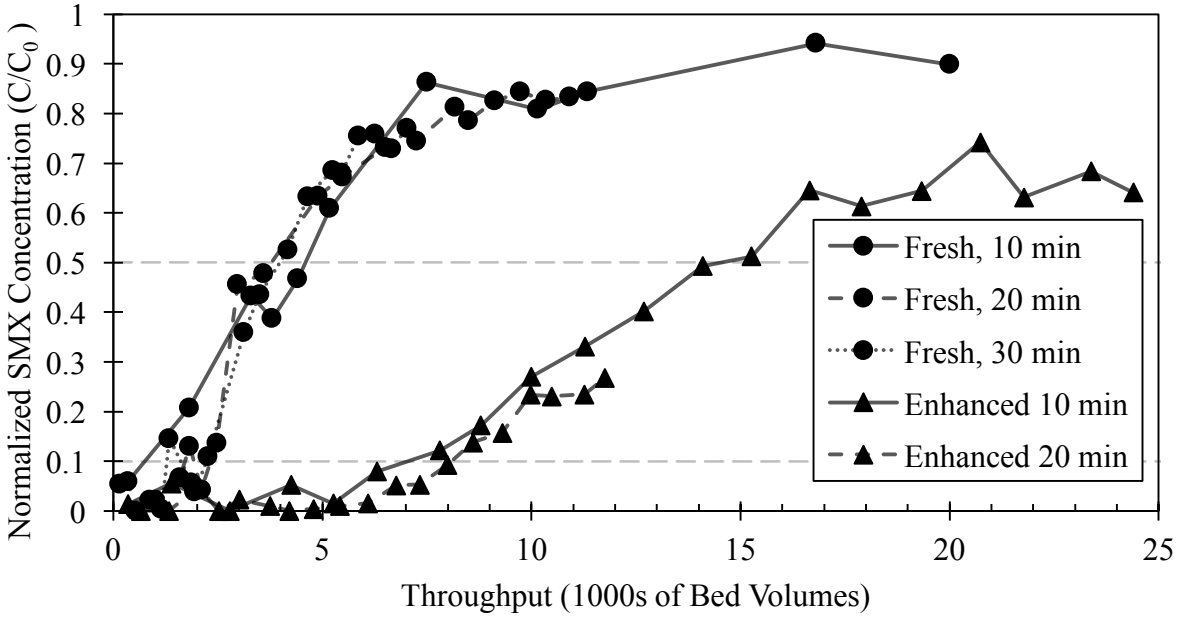

Figure 3.6: Effect of empty bed contact time ($EBCT_{LC}$) on SMX breakthrough for fresh and enhanced biochar.

TOC Breakthrough for Fresh and Regenerated Adsorbents

At an average influent TOC concentration of 4.18 mg/L, TOC broke through beyond 80% within the first 2000 bed volumes for fresh, regenerated, and enhanced biochar, as shown at different EBCTs in Figure 3.7 A, B, and C. Fresh and regenerated biochar performed similarly, but enhanced biochar broke through slightly sooner. On a basis of mass adsorbed, fresh and regenerated char performed similarly, while enhanced biochar adsorbed significantly less, due to its rapid approach to 100% breakthrough.

A)

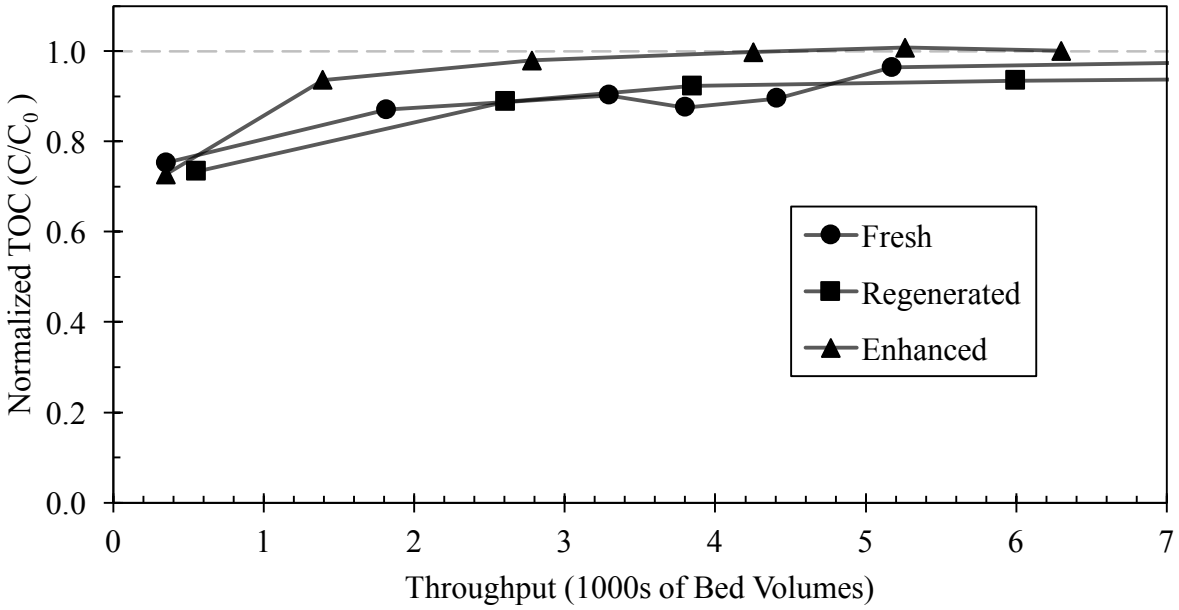

B)

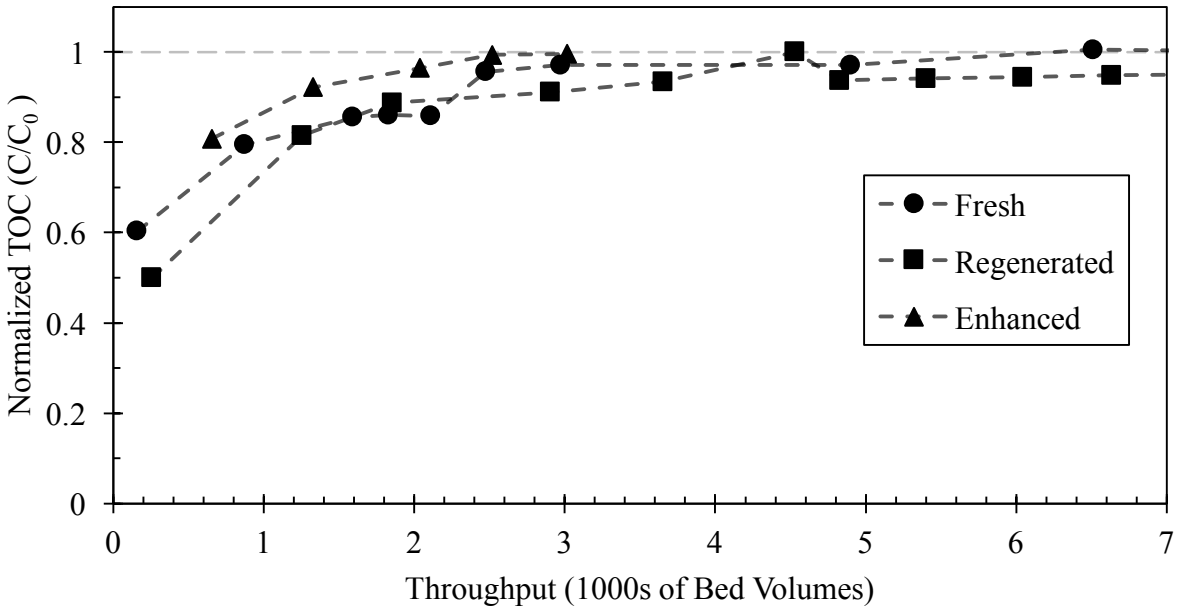

C)

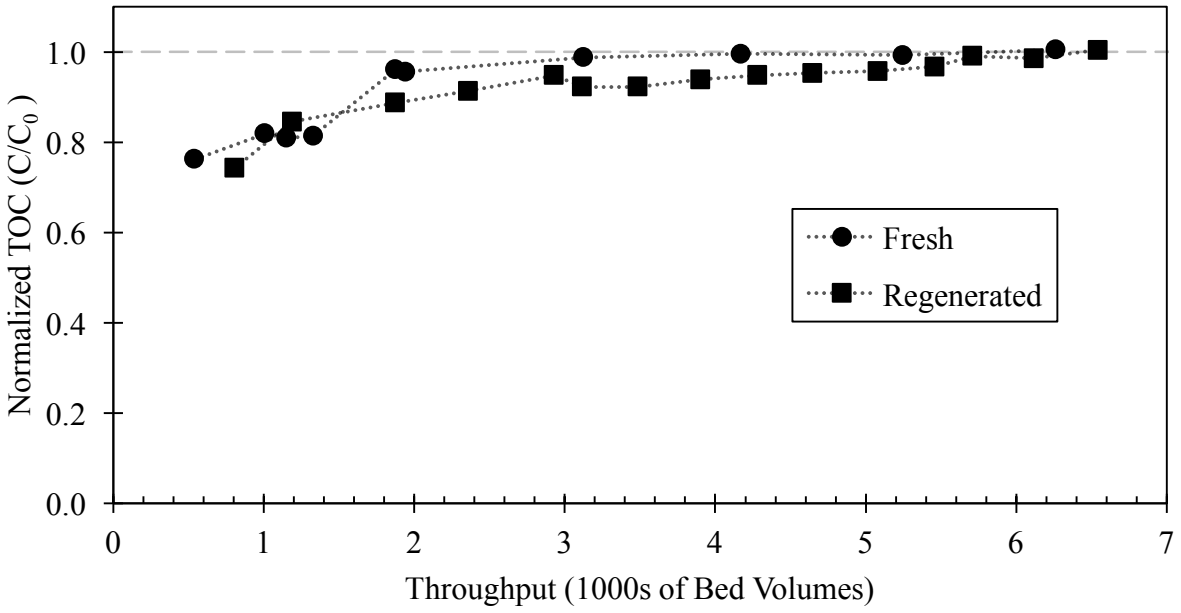

Figure 3.7: TOC breakthrough for various biochars with empty bed contact times ($EBCT_{LC}$) of A) 10 minutes, B) 20 minutes, and C) 30 minutes.

Effect of Empty Bed Contact Time on TOC Breakthrough

The TOC breakthrough data for fresh biochar across different EBCTs are shown in Figure 3.8. The data for regenerated and enhanced char are shown in Figure 3.9. These both suggest no effect of empty bed contact time on adsorption of TOC by biochar.

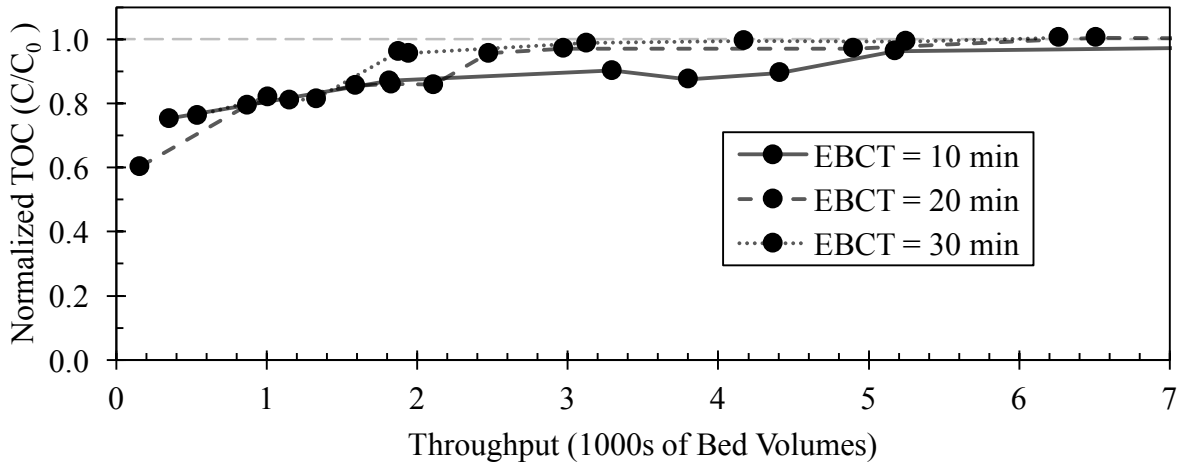

Figure 3.8: TOC breakthrough for fresh biochar with three empty bed contact times ($EBCT_{LC}$).

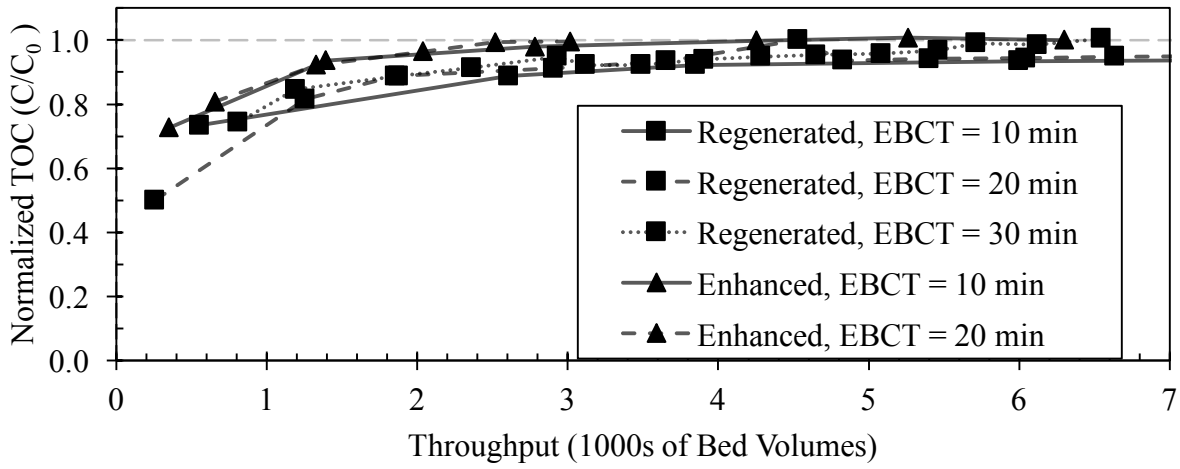

Figure 3.9: TOC breakthrough for regenerated and enhanced biochar with different empty bed contact times ($EBCT_{LC}$).

UVA_{254} Breakthrough for Fresh, Fouled, and Regenerated Adsorbents

UVA, measured at a wavelength of 254 nm, was recorded for all RSSCTs that were conducted. The average influent UVA_{254} was 0.100 cm^{-1}. This breakthrough data is presented for EBCTs of 10 minutes, 20 minutes, and 30 minutes in Figure 3.10 A, B, and C, respectively. A(i) and A(ii) show different scales. The relative performance of the adsorbents closely matched the relative performance observed in SMX breakthrough. Fouled biochar had the lowest adsorption capacity as measured by UVA_{254}, followed by fresh biochar. Chars that had been treated with a thermal regeneration or enhancement step exhibited a higher capacity for adsorbing the aromatic compounds represented by UVA_{254}. However, the effect of the second thermal regeneration cycle were less clear than for SMX adsorption. All biochars were significantly outperformed by activated carbon. The UVA_{254} breakthrough curves were quantified using the bed volumes to 80% UVA_{254} breakthrough, $BV_{80,\,UVA}$. These chosen values are reported in Table 3.1. For biochar, they were highly correlated with the bed volumes to 10% and 50% SMX breakthrough, with R^2 values of 0.94 and 0.87, respectively, when the y-intercept was set to zero. This correlation is visually represented in Figure 3.11, and encourages the notion that UV absorbance at 254nm may have predictive value for biochar performance in future tests, since UVA is much easier to measure than synthetic organic contaminant concentrations. However, the relationship developed for biochar over-predicted throughput to 10% SMX breakthrough in AC by 53%.

A) (i)

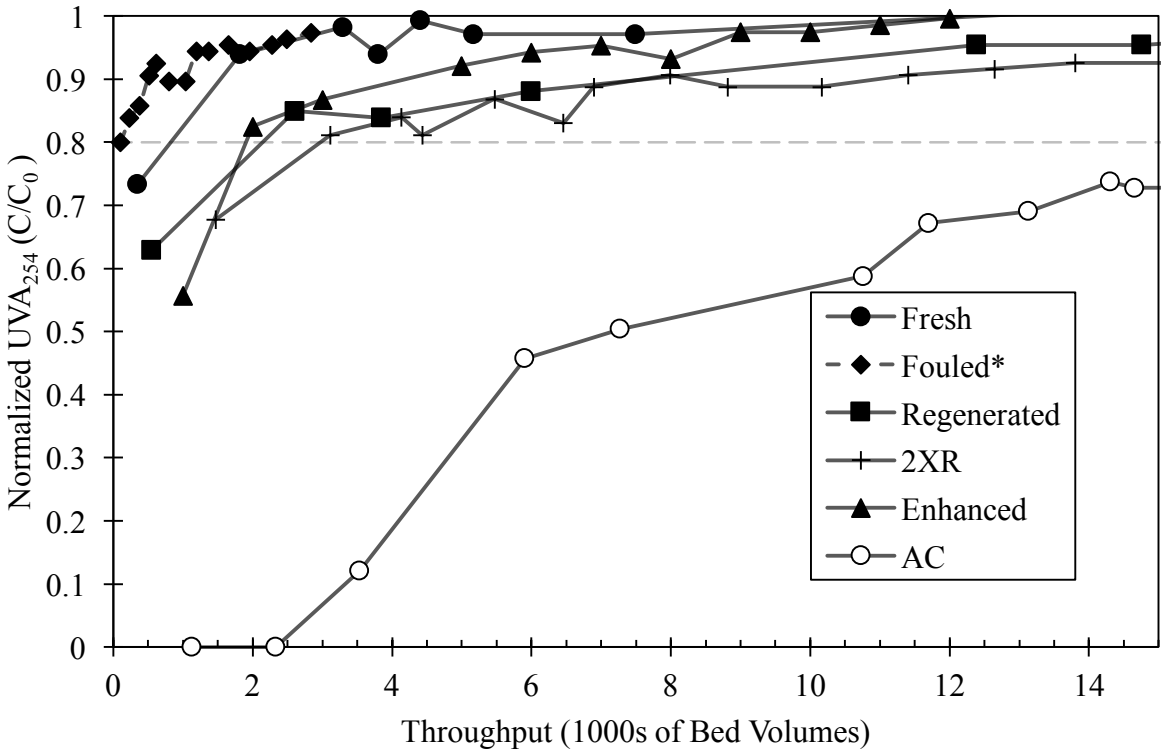
Normalized UVA254 (C/C0)
Throughput (1000s of Bed Volumes)
Fresh
Fouled*
Regenerated
2XR
Enhanced
AC

(ii)

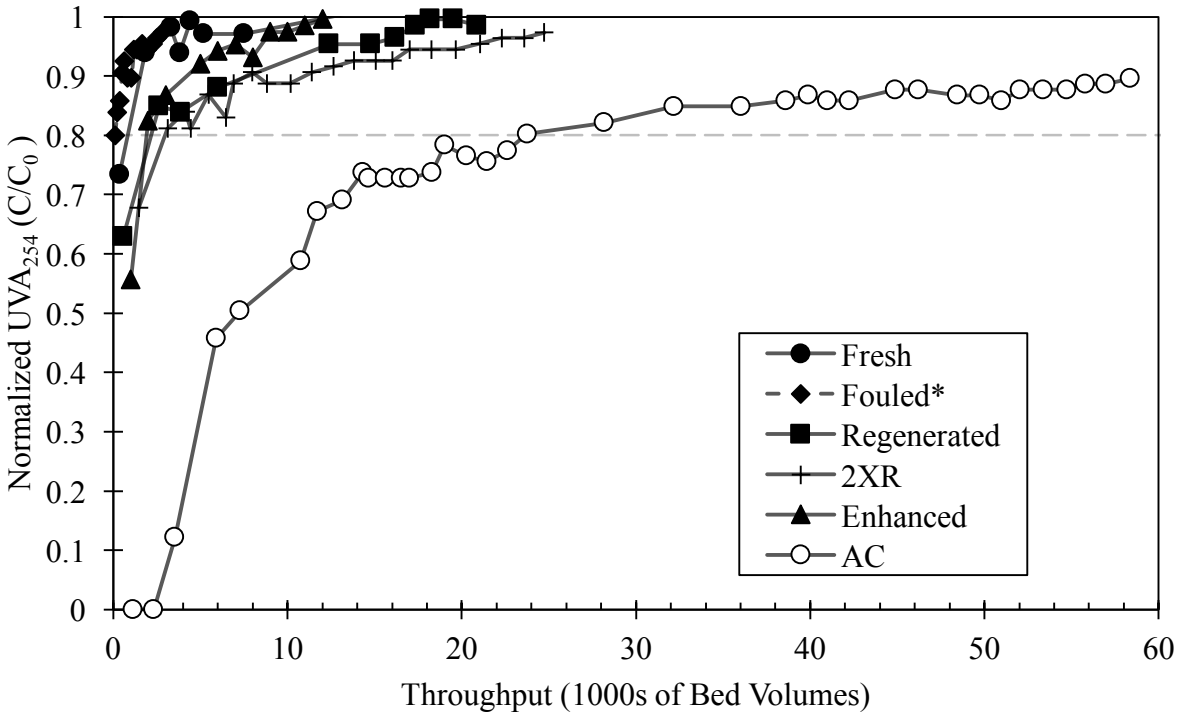
Normalized UVA254 (C/C0)
Throughput (1000s of Bed Volumes)
Fresh
Fouled*
Regenerated
2XR
Enhanced
AC

B)

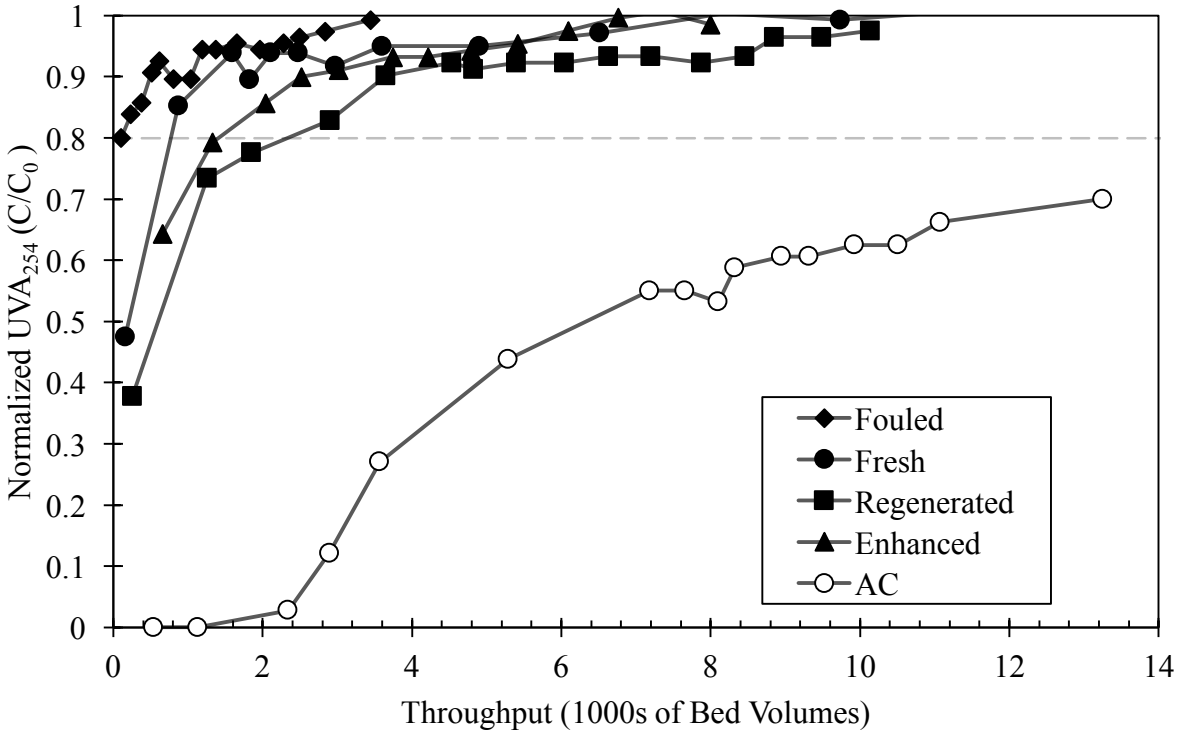

C)

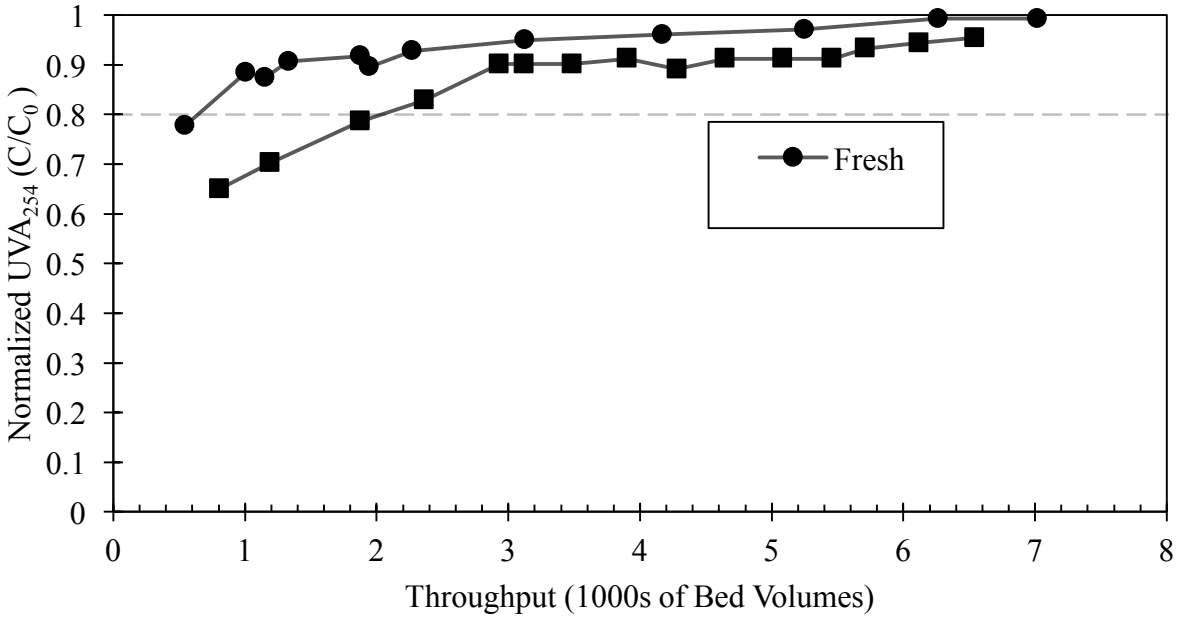

Figure 3.10: UVA_{254} breakthrough for various adsorbents with empty bed contact times ($EBCT_{LC}$) of A)-(i) and -(ii) 10 minutes B) 20 minutes, and C) 30 minutes.

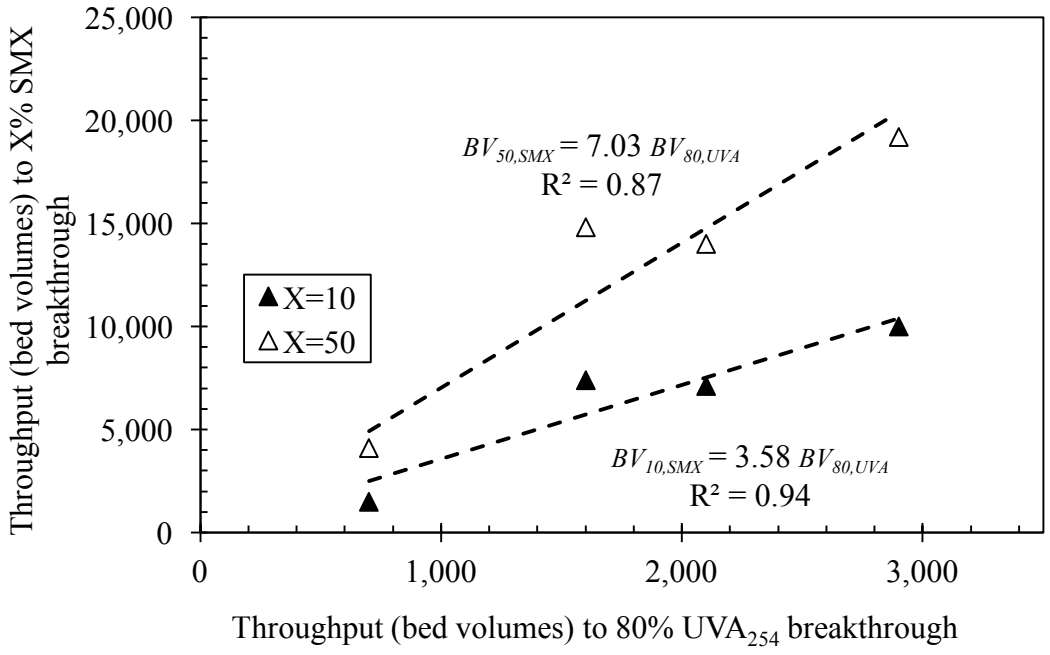

Figure 3.11: Correlation between throughput to 80% UVA_{254} breakthrough and throughput to 10% or 50% SMX breakthrough.

Effect of EBCT on UVA_{254} Breakthrough

The effect of EBCT on UVA_{254} breakthrough is presented for fresh biochar, regenerated biochar, and activated carbon in Figure 3.12, and for enhanced biochar in Figure 3.13. Fresh and regenerated biochar show negligible effects of EBCT. Activated carbon shows marked improved performance at shorter EBCT. Enhanced biochar follows this same trend.

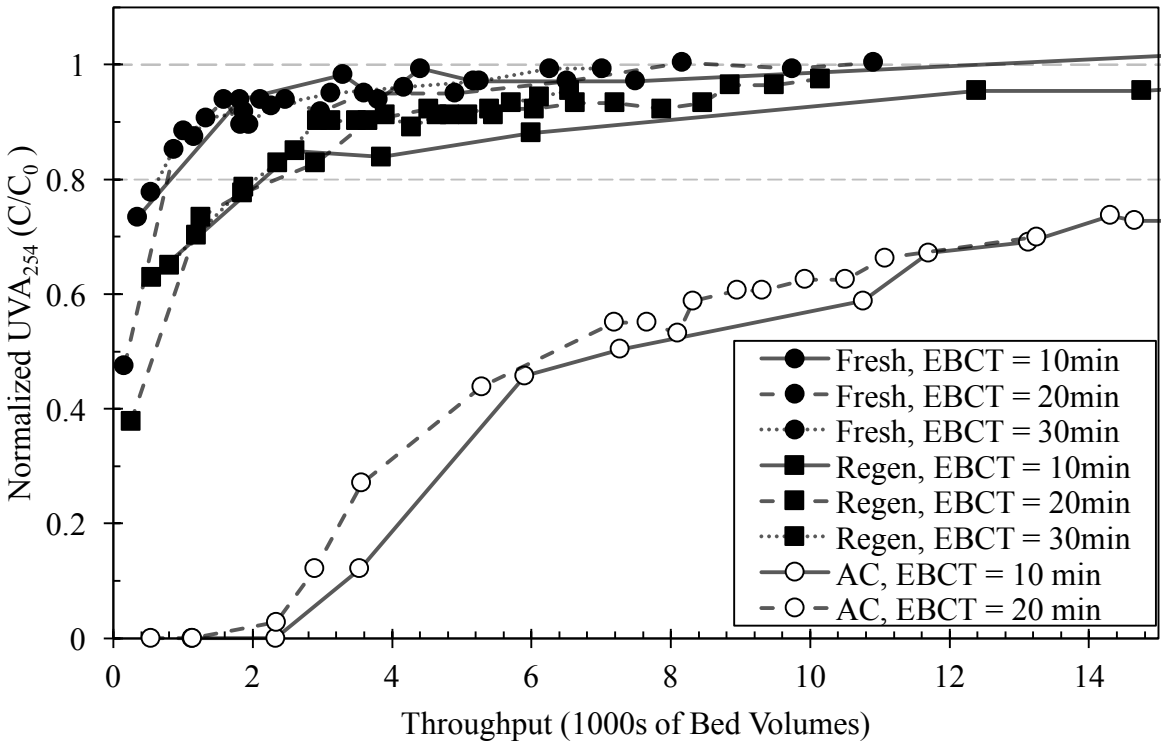

Figure 3.12: UVA_{254} breakthrough for various adsorbents with different empty bed contact times ($EBCT_{LC}$).

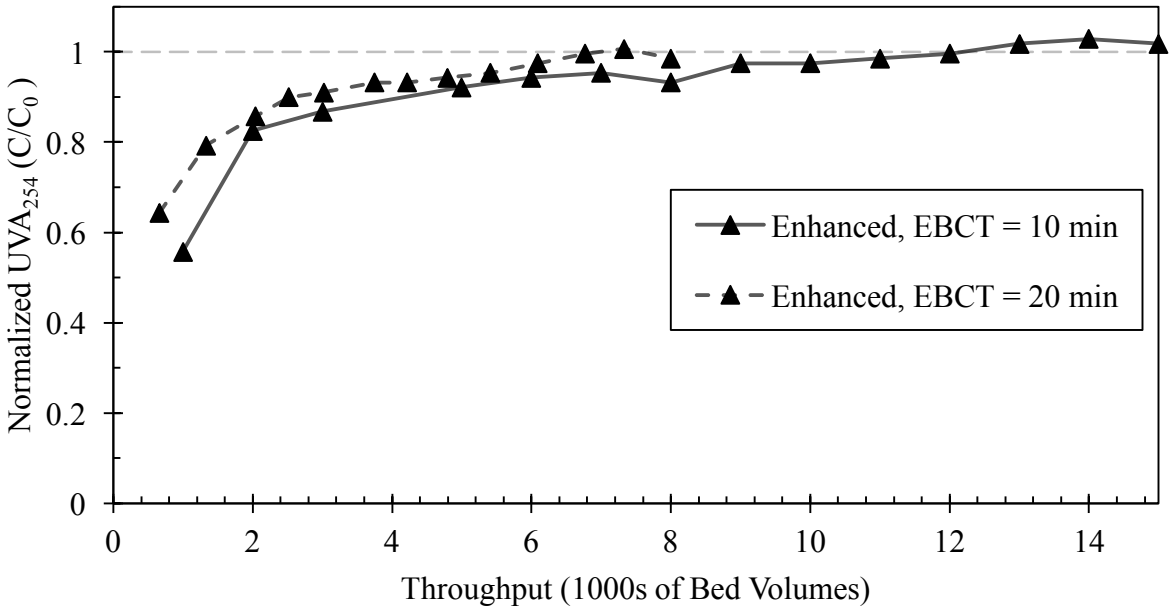

Figure 3.13: UVA_{254} breakthrough for enhanced biochar with two different empty bed contact times ($EBCT_{LC}$).

Comparison of UVA_{254} and TOC Breakthrough

A comparison of UVA_{254} breakthrough to TOC breakthrough for some biochars at 10, 20, and 30 minute EBCTs is shown in Figure 3.14 A, B, and C. UVA_{254} is more strongly adsorbed for regenerated and enhanced biochars at all EBCTs, but this trend seems to be reversed for fresh biochar. TOC breakthrough occurred before UVA_{254} breakthrough with the enhanced and regenerated biochar, while UVA_{254} breakthrough occurred prior to TOC breakthrough for the fresh biochar.

A)

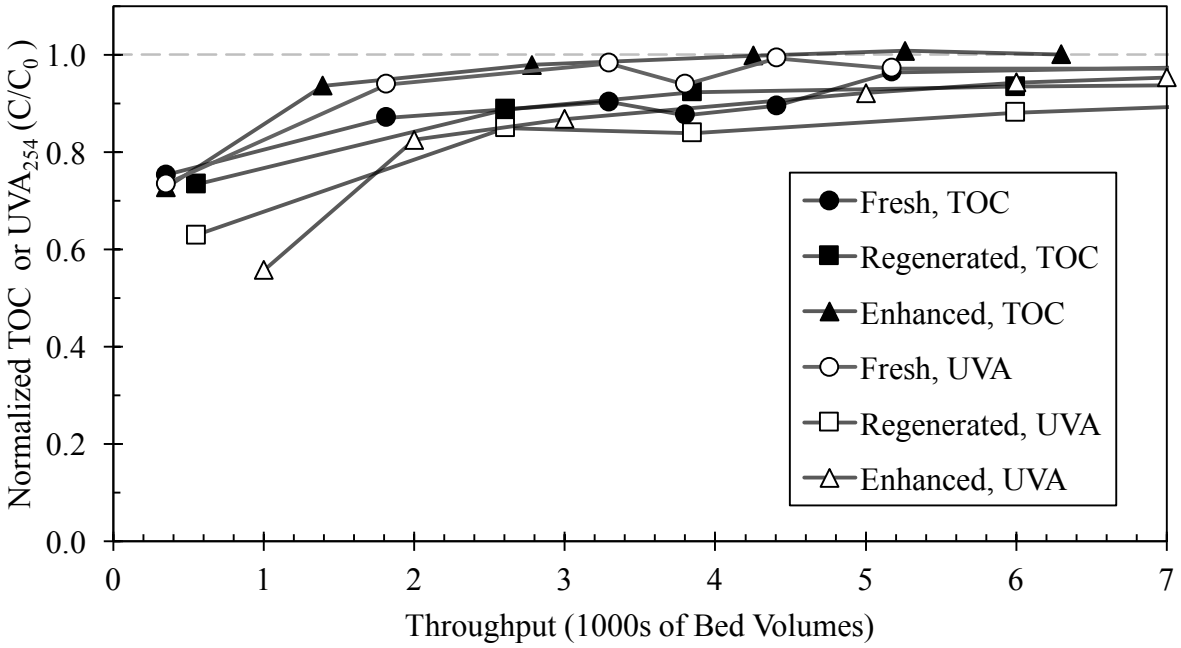

B)

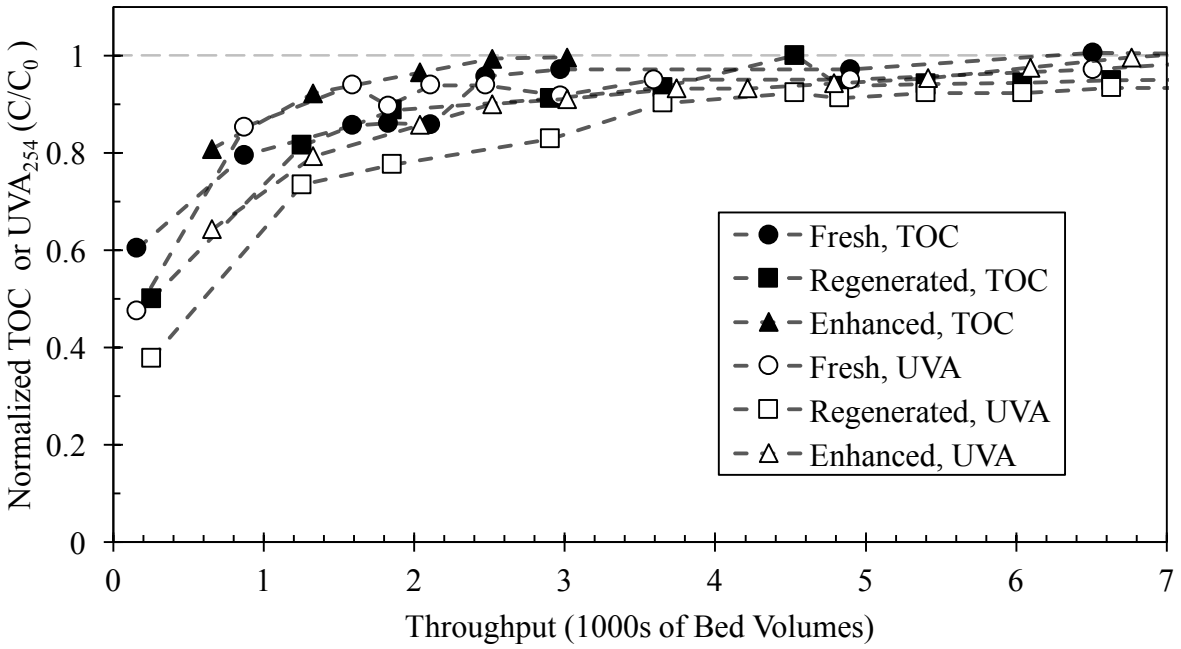

C)

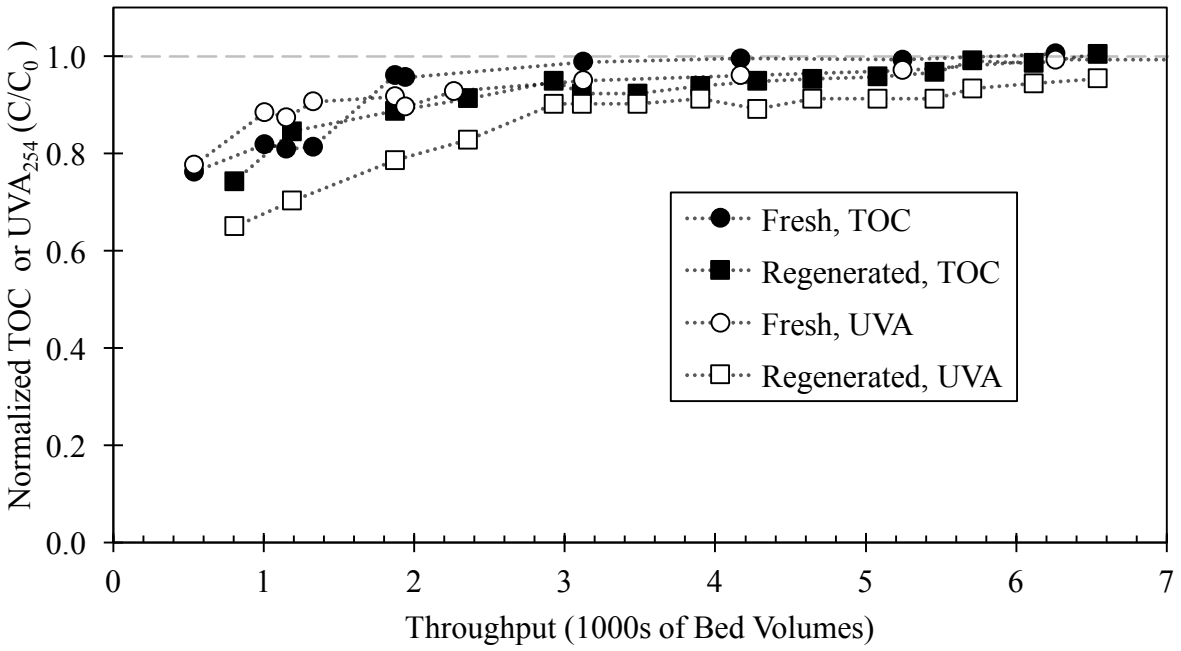

Figure 3.14: Comparison of TOC and UVA_{254} breakthrough for various biochars at empty bed contact times ($EBCT_{LC}$) of A) 10 minutes, B) 20 minutes, and C) 30 minutes.

Particle Size Distribution of Biochars

RSSCT breakthrough curves for removal of trace organics by GAC have been shown to depend on particle size when DOM is present (41). Larger particles are fouled by DOM to a greater extent than smaller ones, and so it is reasonable to expect that a decrease in particle size during drying and thermal regeneration, even within the range of the 100 mesh and 200 mesh sieves, could contribute to the observed increase in adsorption capacity. The particle size distribution of five chars was characterized using a Mastersizer Hydro SM2000(a), which works by analyzing the pattern of light scattered by a representative sample of the char (42). The overlaid cumulative particle size distribution functions are shown in Figure 3.15. Characteristic numbers of the particle size distribution are shown in Table 3.2. These characteristics are defined in the Appendix. The chars had nearly identical particle size distributions, which suggests that a decrease in particle size as described above did not significantly occur during the drying and thermal regeneration processes.

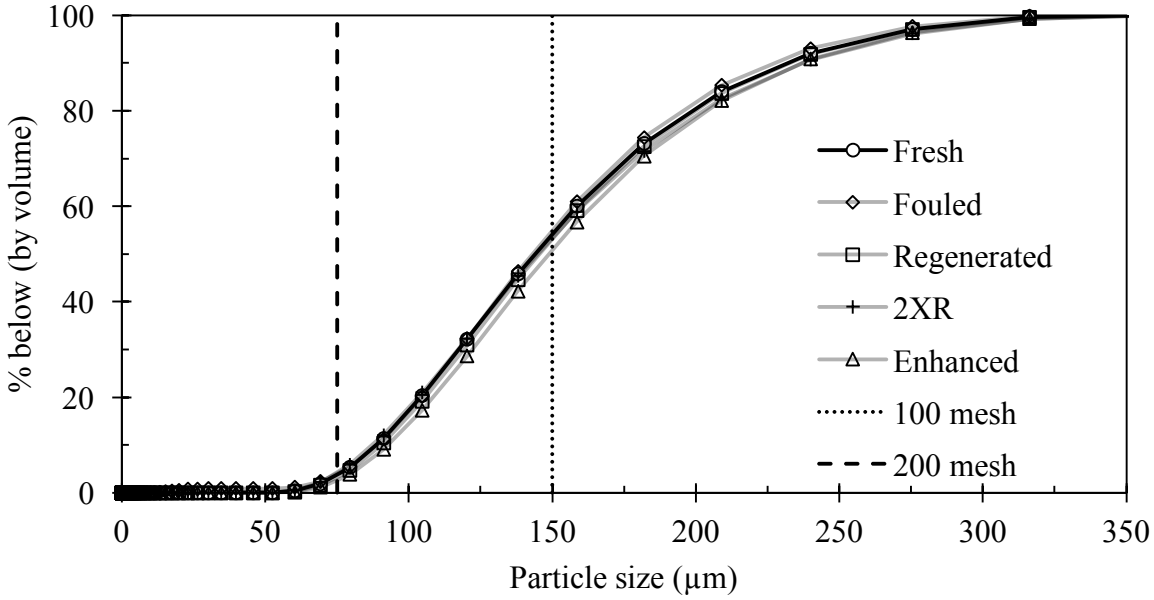

Figure 3.15: Cumulative distribution function of char particle size. Vertical lines indicate the nominal opening size in the upper (100 mesh) and lower (200 mesh) sieves used to produce the chars.

Table 3.2: Particle size distribution parameters

Sample	Span [µm]	D [4, 3], Volume weighted mean [µm]	Uniformity [unitless]	D_{10} [µm]	D_{50} [µm]	D_{90} [µm]	D_{60}* [µm]	C_U, Coefficient of Uniformity [unitless]
Fresh	0.99	153	0.30	89	144	231	159	1.78
Fouled	0.96	151	0.30	89	143	226	157	1.76
Regenerated	0.97	154	0.30	91	145	231	160	1.77
2XR	1.03	155	0.32	88	145	237	161	1.84
Enhanced	0.96	158	0.30	93	149	236	164	1.76

*D_{60} interpolated from Figure 3.15 data.

The opening sizes of standard 100 mesh and 200 mesh sieves, which were used to generate the adsorbent media for the RSSCTs in the present study, are also shown in Figure 3.15. These sizes are 150 µm and 75 µm, respectively. More than 50% of the volume of the samples analyzed was composed of particles larger than the top sieve, despite passing through that sieve in order to be included in the analysis. A possible explanation is that many of the particles are

irregularly shaped. It is conceivable that such a particle could pass though the openings in the top sieve on its shortest axis, but would register as a larger particle in the Mastersizer analysis.

BET Surface Area Analysis

The measured BET surface area of each biochar sample, along with BET surface area reported from the literature of the activated carbon that was used are shown in Table 3.3. After thermal regeneration, the char exhibited a 33% increase in surface area if it had been fouled prior to thermal regeneration, and a 29% increase if it had not been previously fouled. The second cycle of regeneration led to a further 11% increase in surface area. This indicates that the thermal regeneration process is creating or opening access to new surface area, rather than just cleaning previously available surface area. This could indicate that reheating the biochar allows the pyrolysis process to continue, further developing the pore structure beyond what was achieved during the initial 2 hour hold time. Kearns et al. observed an effect of pyrolysis duration on adsorption capacity of biochar, although the only direct comparison was between 4 hours and 4 days of pyrolysis time (20). The increase in surface area could also be due to steam activation owing to residual water in the pores of the biochar when it is reheated, or some level of air activation due to the air that is initially present in the crucible.

The biochar that had been fouled by DOM and SMX did not exhibit a decrease in BET surface area, which could have been an artifact of the method, as the biochar sample may let out gases prior to the adsorption of nitrogen gas at a low temperature. A decrease in surface area due to fouling has been observed in activated carbon used at the full scale (43). This effect could also be missing from the present study because the fouling column was not in operation for long enough to adequately model biological activity, which is the case for RSSCTs in general (15).

Table 3.3: Measured and reported BET surface areas of adsorbents

Sample	BET Surface Area (m^2/g)
Fresh	376 ± 9
Fouled	385 ± 9
Regenerated	500 ± 12
2XR	554 ± 12
Enhanced	485 ± 11
Norit 1240 GAC(44)	1175

As shown in Figure 3.16, the BET surface area of the char samples is very highly correlated with the observed breakthrough of SMX at both 10% and 50% of influent concentrations, with an R^2 value of 0.99 and 0.98, respectively. This indicates that the improvement in adsorption capacity observed in the biochar can be attributed to increases in surface area, and is likely not significantly affected by changes in surface chemistry or particle size. Based on the x-axis intercept (BET surface area) a surface area of more than 350 m^2/g is needed for any appreciable SMX removal to occur. The relationship under-predicts throughput to 10% SMX breakthrough for AC by 29%.

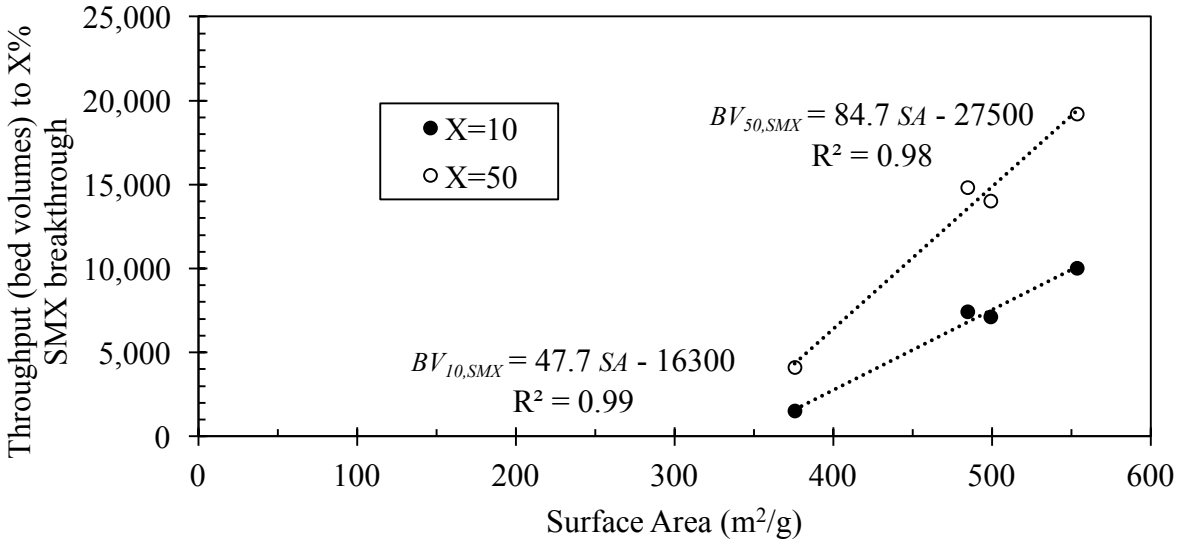

Figure 3.16: Relating 10% and 50% SMX breakthrough to BET surface area

BJH Pore Size Analysis

The Barrett, Joyner, and Halenda (BJH) adsorption average pore diameter was determined for each biochar, and the results are displayed in Figure 3.17, with more detailed information in the Appendix. All biochar samples had an average pore diameter in the lower end of the mesoporous range (2-50nm, or 20-500 Å), and a decrease in average pore diameter was observed for each successive heating step. The regenerated and enhanced biochars exhibited a 6% and 4% decrease in average pore diameter from the fresh biochar average pore diameter, respectively. The second regeneration step led to a further 4% decrease in average pore diameter from that of the regenerated char. This decrease in average pore diameter is strongly correlated with the observed increase in surface area, as shown in Figure 3.18, with an R^2 value of 0.94. This makes sense because the majority of biochar surface area is theorized to reside in micropores (45). Slight changes in pore size distribution were also observed, and the rest of this data is presented in the Appendix.

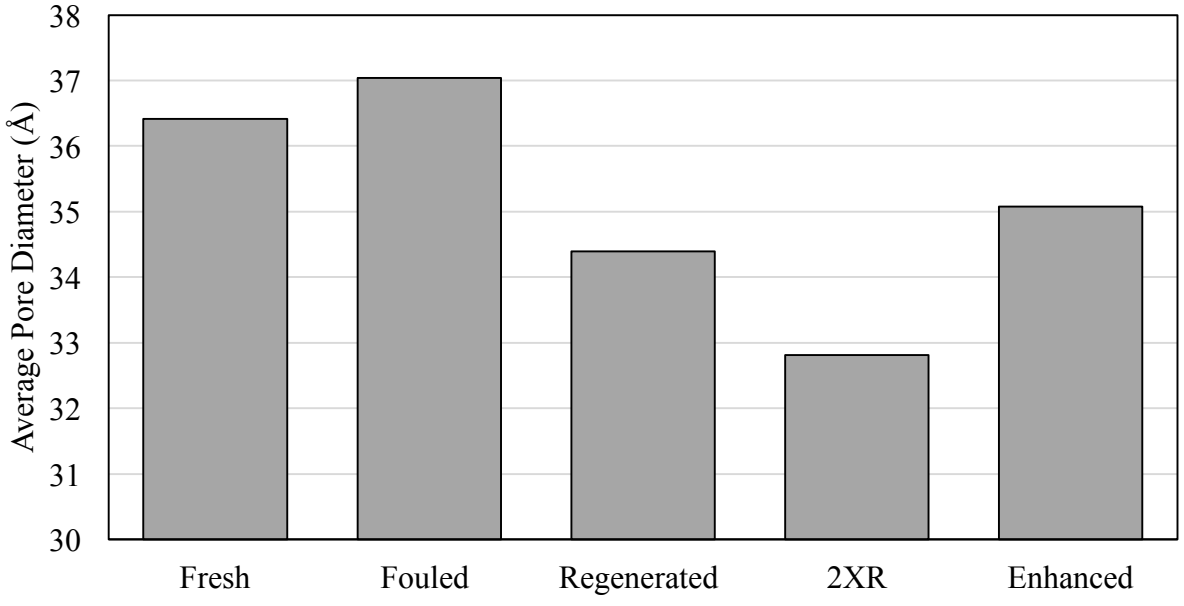

Figure 3.17: BJH Adsorption Average Pore Diameter (4V/A) for different biochars

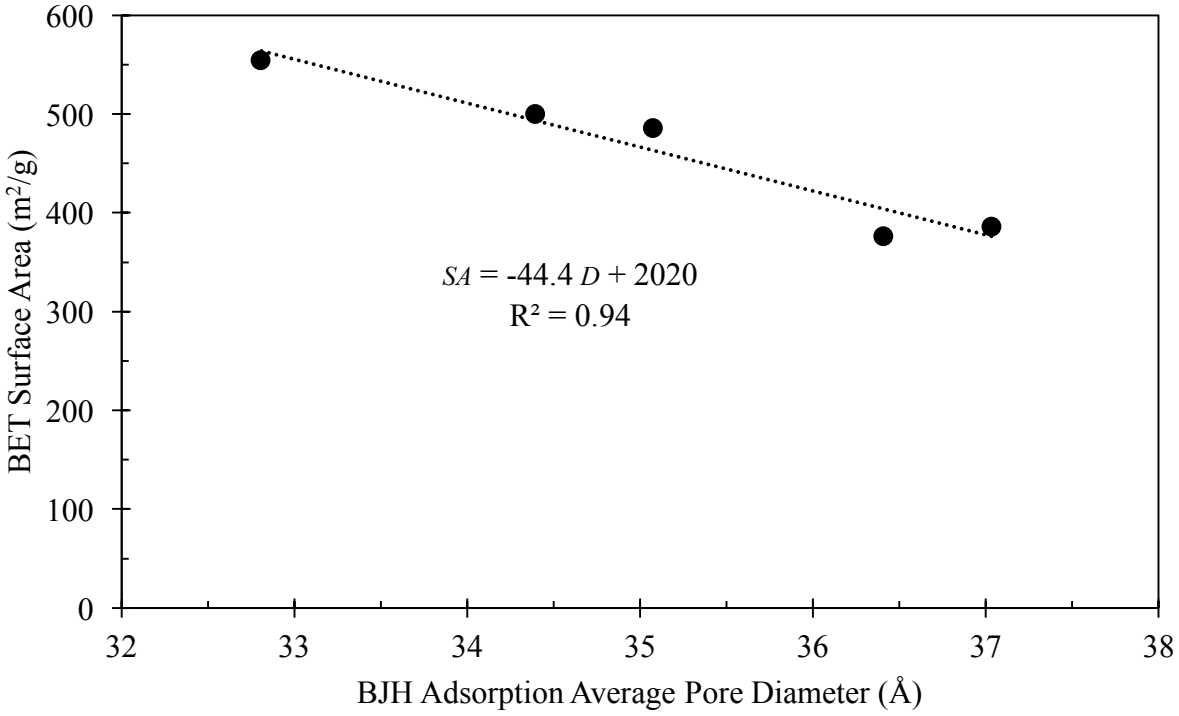

Figure 3.18: Relationship between BET surface area and BJH adsorption average pore diameter

4. CONCLUSION

Heating biochar in a second semi-oxic step at a lower temperature than that originally used to generate the char resulted in a dramatic improvement in column adsorption capacity, even when operated in the presence of DOM. This was quantified by a fourfold increase in the bed volumes to 10% breakthrough of sulfamethoxazole, and nearly fourfold increase in bed volumes to 50% breakthrough. DOM adsorption capacity was also improved. This increase in adsorption capacity was strongly correlated with an observed increase in BET surface area, and was still significant even after accounting for the decrease in mass of char during the heating step of 15 to 20%. The improvement in adsorption and increase in surface area was repeatable for multiple cycles of fouling and regeneration, although the further increase in adsorption capacity in the second regeneration cycle was counteracted by the 25% loss of char mass. While the adsorption capacity of biochar for SMX in the presence of DOM was greatly improved by the second heating step, it does still not approach the capacity of activated carbon in column mode. The average pore diameter of the biochar decreased with each cycle of thermal regeneration, and was negatively correlated with surface area. A positive effect of increased EBCT on SMX adsorption capacity was observed after the regeneration/enhancement heating step, and for activated carbon, but not for fresh biochar. A change in particle size distribution was not observed due to the reheating process, although more than half of the particles were measured to be larger than the expected maximum size of 150 μm.

This process was originally termed thermal regeneration, because the goal was not to further develop the pore structure of the char, but to remove the adsorbed compounds from the internal surfaces of the char, and regain adsorption capacity. However, the observed increase in adsorption capacity, along with an increase in BET surface area both suggest that this semi-oxic

heating step is developing new pore structure within the biochar, and so is therefore more of a reactivation rather than regeneration process. This may be due to residual water inside the pores of the char, or the small amount of air that is present in the crucible as heating occurs. Air (re)activation or thermal (re)activation may be a more appropriate term for the process that was conducted.

Future Investigation

Further research should be conducted on the mechanism of regeneration and/or (re)activation that occurred when biochar was reheated with limited access to oxygen. BET surface area and SOC adsorption capacity should be characterized for chars that have been generated at varying durations in order to illuminate the effect of pyrolysis duration, and separate it from the potential effect of cooling the char to room temperature and raising the temperature again, as was done in the present study. The same characterizations should also be conducted for chars that undergo the second heating step in an inert atmosphere in order to assess whether air activation occurred. Additionally, the effect of temperature during this second step on the adsorption capacity of the biochar should be investigated. Lower regeneration temperatures led to higher mass yields in the present study, and the peak temperature of pyrolysis has been shown to have a significant effect on adsorption capacity of biochar, with lower temperatures yielding worse-performing chars (20,11). It is reasonable to assume that peak regeneration temperature has an effect on adsorption capacity as well, and there is likely to be an optimum temperature at which to conduct this treatment in order to maximize overall adsorption capacity, not just specific adsorption capacity. Field applicability of this technique is also an area of research with many unanswered questions.

5. REFERENCES

1. Schwarzenbach RP, Gschwend PM, Imboden DM. Environmental Organic Chemistry. John Wiley & Sons; 2005. 1330 p.

2. Daughton CG, Ternes TA. Pharmaceuticals and personal care products in the environment: agents of subtle change? Environ Health Perspect. 1999 Dec;107(Suppl 6):907–38.

3. Daughton CG. PPCPs in the Environment: Future Research — Beginning with the End Always in Mind. In: Kümmerer APDK, editor. Pharmaceuticals in the Environment [Internet]. Springer Berlin Heidelberg; 2004 [cited 2016 Dec 29]. p. 463–95. Available from: http://link.springer.com/chapter/10.1007/978-3-662-09259-0_33

4. Kolpin DW, Furlong ET, Meyer MT, Thurman EM, Zaugg SD, Barber LB, et al. Pharmaceuticals, Hormones, and Other Organic Wastewater Contaminants in U.S. Streams, 1999−2000: A National Reconnaissance. Environ Sci Technol. 2002 Mar 1;36(6):1202–11.

5. Daughton CG. Non-regulated water contaminants: emerging research. Environ Impact Assess Rev. 2004 Oct;24(7–8):711–32.

6. Control of Disinfection By-Products in Drinking Water. J Environ Eng [Internet]. 1061 Issue: object: doi: . /joeedu.1994.120.issue-4, revision: rev:1479389630865-13997:doi:10.1061/joeedu.1994.120.issue-4 [cited 2016 Dec 29];120(4). Available from: http://ascelibrary.org/doi/abs/10.1061/%28ASCE%290733-9372%281994%29120%3A4%28727%29

7. Krasner SW, Weinberg HS, Richardson SD, Pastor SJ, Chinn R, Sclimenti MJ, et al. Occurrence of a New Generation of Disinfection Byproducts. Environ Sci Technol. 2006 Dec 1;40(23):7175–85.

8. US EPA O. Stage 1 and Stage 2 Disinfectants and Disinfection Byproducts Rules [Internet]. [cited 2016 Dec 29]. Available from: https://www.epa.gov/dwreginfo/stage-1-and-stage-2-disinfectants-and-disinfection-byproducts-rules

9. Stackelberg PE, Furlong ET, Meyer MT, Zaugg SD, Henderson AK, Reissman DB. Persistence of pharmaceutical compounds and other organic wastewater contaminants in a conventional drinking-water-treatment plant. Sci Total Environ. 2004 Aug 15;329(1–3):99–113.

10. Westerhoff P, Yoon Y, Snyder S, Wert E. Fate of Endocrine-Disruptor, Pharmaceutical, and Personal Care Product Chemicals during Simulated Drinking Water Treatment Processes. Environ Sci Technol. 2005 Sep 1;39(17):6649–63.

11. Shimabuku KK, Kearns JP, Martinez JE, Mahoney RB, Moreno-Vasquez L, Summers RS. Biochar sorbents for sulfamethoxazole removal from surface water, stormwater, and wastewater effluent. Water Res. 2016 Jun 1;96:236–45.

12. Phillips PJ, Chalmers AT, Gray JL, Kolpin DW, Foreman WT, Wall GR. Combined Sewer Overflows: An Environmental Source of Hormones and Wastewater Micropollutants. Environ Sci Technol. 2012 May 15;46(10):5336–43.

13. Joshua Perry Kearns. Biochar adsorbent for control of synthetic organic contaminants in affordable decentralized water treatment [Ph.D.]. [United States -- Colorado]: University of Colorado Boulder; 2016.

14. Frederik T. Weiss, Marianne Leuzinger, Christian Zurbrügg, Rik I.L. Eggen. Chemical Pollution in Low- and Middle-Income Countries. Überlandstrasse 133, 8600 Dübendorf, Switzerland: EAWAG; 2016.

15. Sontheimer H, Crittenden JC, Summers RS. Activated Carbon for Water Treatment. 2nd Edition. Karlsruhe, Germany: DVGW-Forschungsstelle; 1988. 722 p.

16. John C. Crittenden, Hand DW, Arora H, Lykins Jr. BW. Design Considerations for GAC Treatment of Organic Chemicals. Am Water Work Assoc J. 1987 Jan 1;79(1):74–82.

17. Corwin CJ, Summers RS. Controlling trace organic contaminants with GAC adsorption. Am Water Works Assoc J. 2012 Jan;104(1):43–4.

18. Kennedy AM, Reinert AM, Knappe DRU, Ferrer I, Summers RS. Full- and pilot-scale GAC adsorption of organic micropollutants. Water Res. 2015 Jan 1;68:238–48.

19. Kearns JP, Shimabuku KK, Mahoney RB, Knappe DRU, Summers RS. Meeting multiple water quality objectives through treatment using locally generated char: improving organoleptic properties and removing synthetic organic contaminants and disinfection by-products. J Water Sanit Hyg Dev. 2015 Sep 1;5(3):359–72.

20. Kearns JP, Wellborn LS, Summers RS, Knappe DRU. 2,4-D adsorption to biochars: Effect of preparation conditions on equilibrium adsorption capacity and comparison with commercial activated carbon literature data. Water Res. 2014 Oct 1;62:20–8.

21. Kearns JP, Knappe DRU, Summers RS. Synthetic organic water contaminants in developing communities: an overlooked challenge addressed by adsorption with locally generated char. J Water Sanit Hyg Dev. 2014 Sep 1;4(3):422–36.

22. Summers RS, Kim SM, Shimabuku K, Chae S-H, Corwin CJ. Granular activated carbon adsorption of MIB in the presence of dissolved organic matter. Water Res. 2013 Jun 15;47(10):3507–13.

23. Kennedy AM, Summers RS. Effect of DOM Size on Organic Micropollutant Adsorption by GAC. Environ Sci Technol. 2015 Jun 2;49(11):6617–24.

24. R. Scott Summers, Detlef R. U. Knappe, Vernon L. Snoeyink. 14. Adsorption of organic compounds by activated carbon. In: Water Quality and Treatment: A Handbook on Drinking Water. Sixth. American Water Works Association; 2011.

25. Crittenden JC, Reddy PS, Arora H, Trynoski J, Hand DW, Perram DL, et al. Predicting GAC Performance with Rapid Small-Scale Column Tests. Am Water Work Assoc J. 1991 Jan;77–87.

26. Crittenden JC, Trussell RR, Hand DW, Howe KJ, Tchobanoglous G. MWH's Water Treatment: Principles and Design. Third. John Wiley & Sons; 2012. 1704 p.

27. Salvador F, Martin-Sanchez N, Sanchez-Hernandez R, Sanchez-Montero MJ, Izquierdo C. Regeneration of carbonaceous adsorbents. Part I: Thermal Regeneration. Microporous Mesoporous Mater. 2015 Jan 15;202:259–76.

28. Moreno-Castilla C, Rivera-Utrilla J, Joly JP, López-Ramón MV, Ferro-García MA, Carrasco-Marín F. Thermal regeneration of an activated carbon exhausted with different substituted phenols. Carbon. 1995;33(10):1417–23.

29. Suzuki M, Misic DM, Koyama O, Kawazoe K. Study of thermal regeneration of spent activated carbons: Thermogravimetric measurement of various single component organics loaded on activated carbons. Chem Eng Sci. 1978 Jan 1;33(3):271–9.

30. Miguel GS, Lambert SD, Graham NJD. Thermal Regeneration of Granular Activated Carbons Using Inert Atmospheric Conditions. Environ Technol. 2002 Dec 1;23(12):1337–46.

31. Aqueous Solutions. JRO Gasifier and Retort Char System [Internet]. 2010 [cited 2017 Jan 16]. Available from: http://www.aqsolutions.org/images/2010/06/JRO-handbook.pdf

32. Hirsch R, Ternes T, Haberer K, Kratz K-L. Occurrence of antibiotics in the aquatic environment. Sci Total Environ. 1999 Jan 12;225(1–2):109–18.

33. Heberer T. Occurrence, fate, and removal of pharmaceutical residues in the aquatic environment: a review of recent research data. Toxicol Lett. 2002 May 10;131(1–2):5–17.

34. National Center for Biotechnology Information. CID=5329. In: PubChem Compound Database [Internet]. [cited 2017 Jan 18]. Available from: https://pubchem.ncbi.nlm.nih.gov/compound/5329

35. Boreen AL, Arnold WA, McNeill K. Photochemical Fate of Sulfa Drugs in the Aquatic Environment: Sulfa Drugs Containing Five-Membered Heterocyclic Groups. Environ Sci Technol. 2004 Jul 1;38(14):3933–40.

36. Al-Ahmad A, Daschner FD, Kümmerer K. Biodegradability of Cefotiam, Ciprofloxacin, Meropenem, Penicillin G, and Sulfamethoxazole and Inhibition of Waste Water Bacteria. Arch Environ Contam Toxicol. 1999 Aug 1;37(2):158–63.

37. Christopher J. Corwin, R. Scott Summers. Controlling trace organic contaminants with GAC adsorption. J - Am Water Works Assoc. 2012;E36–47.

38. Bucheli TD, Bachmann HJ, Blum F, Bürge D, Giger R, Hilber I, et al. On the heterogeneity of biochar and consequences for its representative sampling. J Anal Appl Pyrolysis. 2014 May;107:25–30.

39. Crittenden J, Berrigan J, Hand D, Lykins B. Design of Rapid Fixed-Bed Adsorption Tests for Nonconstant Diffusivities. J Environ Eng. 1987 Apr 1;113(2):243–59.

40. Standard Practice for the Prediction of Contaminant Adsorption On GAC In Aqueous Systems Using Rapid Small-Scale Column Tests. ASTM.

41. Corwin CJ, Summers RS. Scaling Trace Organic Contaminant Adsorption Capacity by Granular Activated Carbon. Environ Sci Technol. 2010 Jul 15;44(14):5403–8.

42. Mastersizer 2000 User Manual [Internet]. Malvern Instruments; 2007 [cited 2016 Dec 17]. Available from: https://www.labmakelaar.com/fjc_documents/mastersizer-2000-2000e-manual-eng1.pdf

43. Newcombe G, Hayes R, Drikas M. Granular activated carbon: Importance of surface properties in the adsorption of naturally occurring organics. Colloids Surf Physicochem Eng Asp. 1993 Oct 15;78:65–71.

44. Yapsaklı K, Çeçen F, Aktaş Ö, Can ZS. Impact of Surface Properties of Granular Activated Carbon and Preozonation on Adsorption and Desorption of Natural Organic Matter. ResearchGate. 2009 Mar 1;26(3):489–500.

45. Lehmann DJ, Joseph S. Biochar for Environmental Management: Science and Technology. Earthscan; 2009. 449 p.

6. APPENDIX

Equations

Equation 1: D_X

$$D_X = diameter\ for\ which\ X\%\ (by\ volume) of\ sample\ is\ composed\ of\ smaller\ particles$$

Equation 2: Span (42)

$$Span = \frac{D_{90} - D_{10}}{D_{50}}$$

Equation 3: Coefficient of Uniformity (15)

$$C_u = \frac{D_{60}}{D_{10}}$$

Equation 4: Uniformity (42)

$$U = \frac{\Sigma v_i |d(v, 0.5) - d_i|}{d(v, 0.5)\Sigma v_i}$$

where $d(v,0.5)$ is the median size of the distribution in terms of volume, and d_i and v_i are respectively the mean diameter of, and result in, size class i.

Equation 5: Volume weighted mean (42)

$$D[m, n] = \left[\frac{\Sigma V_i {d_i}^{m-3}}{\Sigma V_i {d_i}^{n-3}}\right]^{\frac{1}{m-n}}$$

where $m = 4$ and $n = 3$.

Supplementary Data

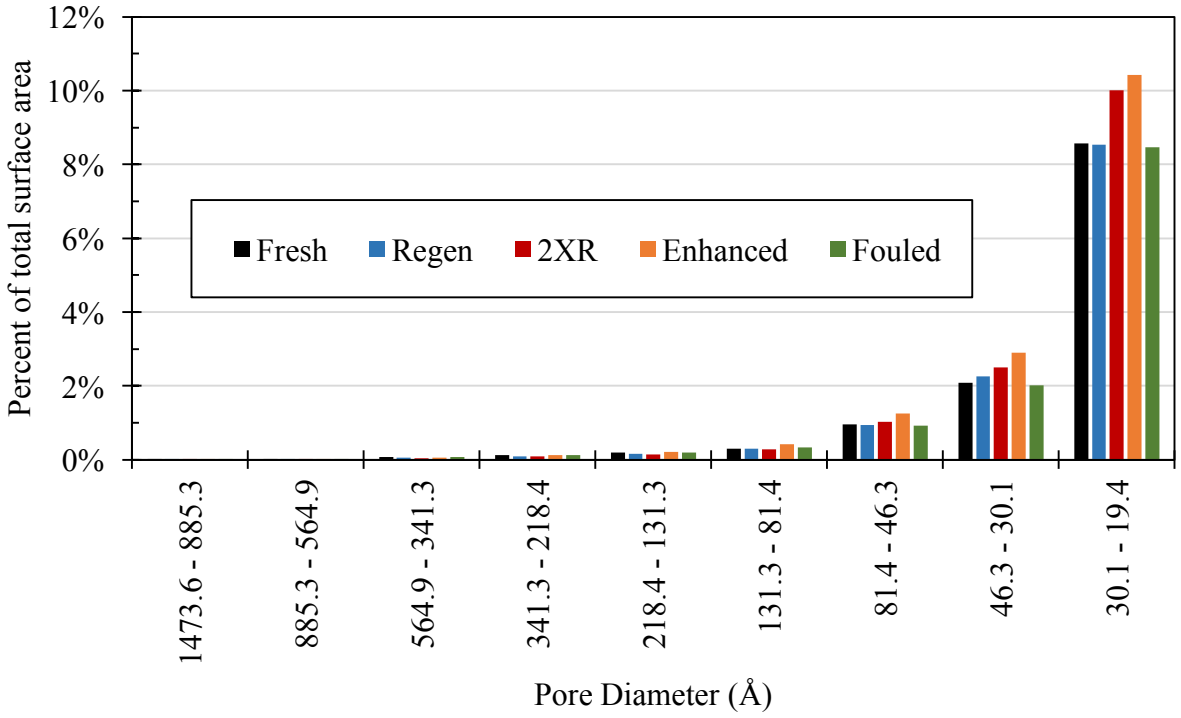

Figure 6.1: BJH pore size distribution of biochars in terms of surface area in a given size range.

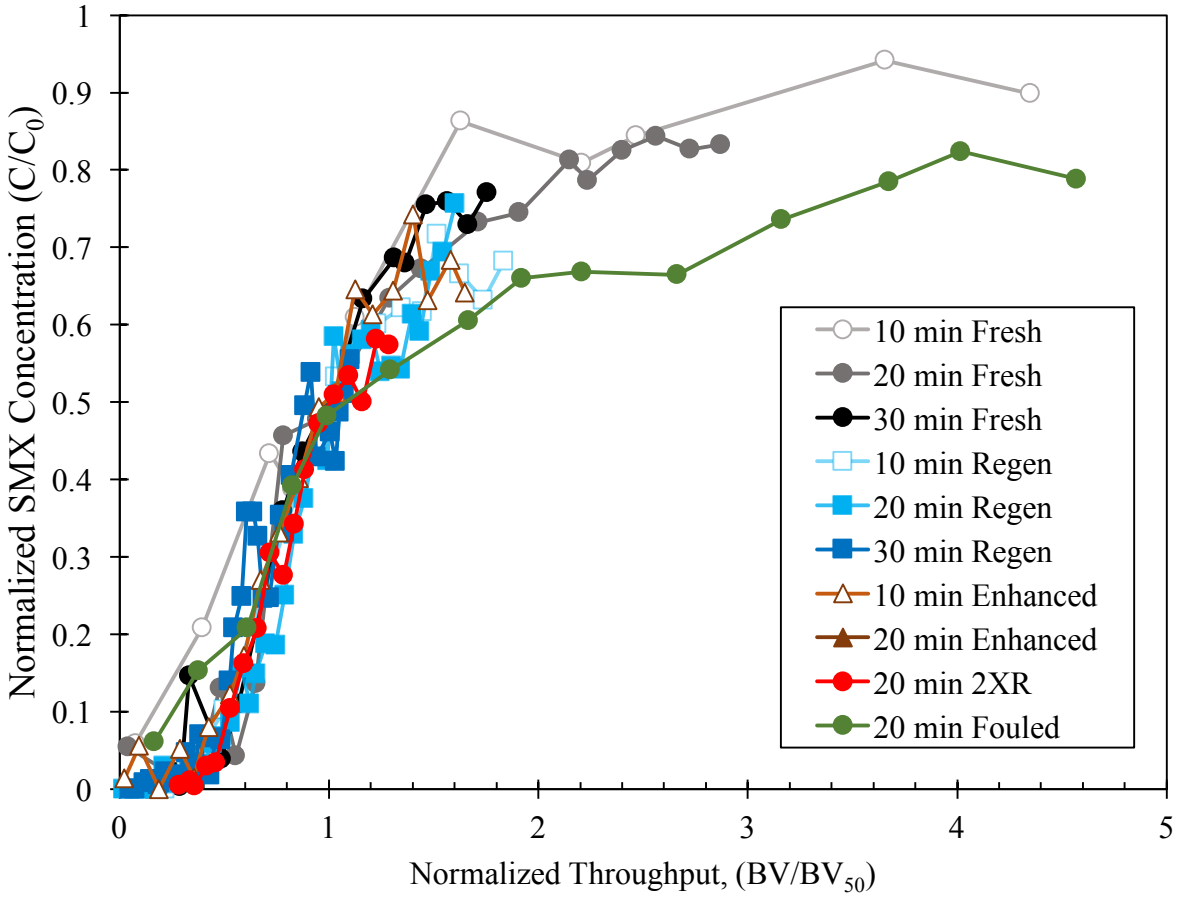

Figure 6.2: Breakthrough of sulfamethoxazole as a function of throughput normalized to BV50. Breakthrough curves exhibit similar shapes for all adsorbents, indicating that the adsorption kinetics are not affected by the regeneration process.

Table 6.1: Total efficiency of regeneration processes, and approximate throughput to 10% and 50% SMX breakthrough and 80% UVA breakthrough for each EBCT and adsorbent. BV_X' values were chosen as representative values for the adsorbent based on inspection, and are also shown in Table 3.1.

Adsorbent	η_{total}	$BV_{10,\,SMX}$ *(bed volumes)*					$BV_{50,\,SMX}$ *(bed volumes)*					$BV_{80,\,UVA}$ *(bed volumes)*			
		EBCT (min)			$BV_{10,\,SMX}'$	$BV_{10,\,SMX}' \times \eta_{total}$	EBCT (min)			$BV_{50,\,SMX}'$	$BV_{50,\,SMX}' \times \eta_{total}$	EBCT (min)			$BV_{80,\,UVA}'$
		10	20	30			10	20	30			10	20	30	
Fresh	1	800	2,000	1,600	1,500	1,500	4,600	3,800	4,000	4,100	4,100	800	800	600	700
Fouled	-	-	150	-	150	-	-	620	-	620	-	-	100	-	100
Regen	0.85	5,900	7,400	8,000	7,100	6,100	12,000	13,600	16,000	14,000	12,000	2,100	2,400	2,000	2,100
2XR	0.64	10,000	-	-	10,000	6,400	19,200	-	-	19,200	12,300	2,900	-	-	2,900
Enhanced	0.80	6,800	8,000	-	7,400	5,900	14,800	-	-	14800	11,900	1,900	1,400	-	1,600
GAC	-	56,000	-	-	56,000	-	-	-	-	-	-	24,000	-	-	24,000

Table 6.2: Pore Size Distribution and Surface Area Characteristics

Sample	BET Surface Area (m^2/g)	BET SA Standard Deviation (m^2/g)	Langmuir Surface Area (m^2/g)	BJH Adsorption cumulative surface area of pores between 17.000 Å and 3000.000 Å diameter (m^2/g)	BJH Desorption cumulative surface area of pores between 17.000 Å and 3000.000 Å diameter (m^2/g)	Adsorption average pore width (4V/A by BET) (Å)	Desorption average pore width (4V/A by BET) (Å)	BJH Adsorption average pore diameter (4V/A) (Å)	BJH Desorption average pore diameter (4V/A) (Å)
Fresh	375.7499	8.6432	496.3021	46.307	37.8783	20.5046	20.6246	36.41	32.097
Fouled	385.383	8.9069	509.1899	46.814	37.8509	20.5289	20.6634	37.037	31.448
Regenerated	499.3928	11.5132	658.3282	61.597	67.3522	20.3781	20.3981	34.397	32.056
2XR	553.5491	12.4668	730.672	78.141	86.5718	20.4042	20.4249	32.809	30.883
Enhanced	484.8114	10.6968	640.2248	74.799	82.7565	20.9425	20.9857	35.078	32.615